

Correlated evolution: models and methods.

G Achaz^{1,2}, JY Dutheil^{3,4}

- 1: UMR7206 Eco-Anthropologie, Université de Paris–CNRS–MNHN, Paris
 - 2: UMR7241 Centre Interdisciplinaire de Recherche en Biologie, Collège de France–CNRS–INSERM, Paris
 - 3: AG Molecular Systems Evolution – Max Planck Institute for Evolutionary Biology, Plön, Germany
 - 4: Institute des Sciences de l'Evolution - Montpellier, Université Montpellier–CNRS–EPHE–IRD, Montpellier, France
- Corresponding author: guillaume.achaz@mnhn.fr

Contents

1	Introduction	3
2	Correlated evolution between traits	5
2.1	Species are not independent	5
2.2	The phylogenetically independent contrasts	6
2.3	Extending the linear model to account for phylogeny	7
2.4	Correlation between discrete traits	10
2.5	Examples of correlated traits	12
2.6	Jointly modeling traits and sequences	13
3	Correlated evolution within genomes	13
3.1	Within genes, between nucleotides	14
3.2	Within proteins, between amino-acids	16
3.3	Within genomes, between genes	20
4	Genetics is also correlated evolution	22
4.1	In individuals	23
4.2	In pedigrees	24
4.3	In the population	25
5	Conclusion	29
6	Acknowledgments	30

1 Introduction

As soon as the word *co-evolution* is dropped, the attention of evolutionary biologists rises. Some pictures illuminating patterns of co-evolution between species such the joint evolution of the beak of the beautiful pollinating hummingbirds and its associated flowers [Kay et al., 2005] or the terrifying arm races between ferocious pathogens and their hosts [Woolhouse et al., 2002]; soon after, many will think about Alice running on the spot with the Red Queen through the looking glass [Van Valen, 1973]. Our fascination about complex evolving entities that are in constant dynamical interactions often lies at the cross-road between Ecology and Evolution, both being arguably parts of the field coined Population Biology [Lewontin, 2004].

There is, however, another common usage of the term *co-evolution*, popular among molecular evolutionary biologists, where the co-evolving entities are not interacting species of an ecological community, but traits of the same individual, species or genome. This chapter reviews a selection of models and methods related to this second meaning. We use equally the terms *co-evolution* and *correlated evolution* to name the joint evolution of two or more traits; *trait* refers to *any* character of individuals, ranging from morphological traits (e.g. height) to genetic variant (e.g. an allele at a locus). We are naturally inclined to accept patterns of co-evolution between the height and the body mass of individuals or, at the molecular level, between paired nucleotides of the same RNA molecule. We show in this review how, once abstracted, the models and methods that have been used to characterize the correlated evolution between morphological traits or between nucleotides share several common features. They are designed in the same general framework and only differ by details of their implementation.

To demonstrate correlated evolution between two traits, one has to reject the statistical independence between the two processes that govern the evolution of the two traits. To do so, one can look at the state of the two traits in many individuals, species or genomes and characterize the co-occurrence or co-abundance of the two traits among the cohort. Alternatively, one can compare the evolutionary paths of the two trait states and scan for signs of co-variations. The hope is that the patterns of correlated evolution is caused by biologically relevant interactions between the two traits. However, as for any pattern of correlation, the non-independence can be indirectly caused by correlations to a third hidden variable. For instance, an environmental variable may drive synchronised changes in several traits that are not interacting directly. As always, *correlation does not imply causation*.

When the evolution of the two traits are actually directly interacting, it is usually the case that their joint mutations have a different impact on fitness than what is expected by the mutation of each one. For example, they can have a synergistic effect when mutating both traits together result in a larger fitness improvement than the sum of each mutation. At the molecular level, interactions between loci, a phenomenon known as epistasis, were the subject of long-standing interests for geneticists [Phillips, 2008]. In its simplest form, let's consider two binary traits. An individual can then have 4 possible trait states: 00, 01, 10, 11. Each of the combination can be associated to a fitness value. The map of all possible combinations of trait states to a fitness value is known as a fitness landscape [Wright, 1932]. For the simple case of 2 traits with two states, the fitness landscape can be easily sketched as in Figure 1.

Depending on which fitness landscape both traits are evolving in, one expects different patterns of correlated evolution. Probably the strongest patterns of co-evolution would arise when only the double mutant is not associated to a fitness loss (Figure 1d). It corresponds to cases of compensation where the second mutation will compensate, or even over-compensate, the first one. In such a case, we would only observe individuals with trait combinations 00 or 11, and more rarely the intermediate states. Similarly, we expect to only witness synchronized mutations in the evolutionary paths of the two traits, where one mutation in a trait is immediately followed by a mutation in the other. Fitness landscapes have fascinated evolutionary biologists (among others) for almost a century and are still nowadays an object of vivid interest [Achaz et al., 2014, Visser and Krug, 2014, Yi and Dean, 2019].

In this chapter, we will first explore models of correlated evolution between continuous and discrete traits (section 1). These models are historically used to characterize how traits are co-varying in the natural world as species evolve through time. We will then continue our journey with models of correlated evolution within genomes (section 2), that have many times been successfully applied to understand co-variations within the same molecule (RNA or proteins), but also at a larger scale to assess co-evolution between different genes or even between regulatory elements and genes. Finally, we will show how standard classical genetics can be rethought in terms of correlated evolution (section 3) between phenotypic trait(s) and molecular trait(s) in the genome.

In this chapter, we review the broad corpus of models and methods that have been developed to study coevolution. We more particularly explain the motivations and basic principles of a few chosen models and their related methodologies. We hope that this review will provide to the readers an original overview

of the field of *correlated evolution* by integrating evolution, genetics, structural biology, statistical physics, modelling and statistics.

2 Correlated evolution between traits

2.1 Species are not independent

Co-evolution is expected to result in correlations of character states when measured in several species. Comparative analysis, therefore, constitutes a natural method of investigation to exhibit coevolving traits. The simple comparative analysis of observed states, however, could be misleading as biological species are not statistically independent. Quite on the contrary, as all species share ancestry, the quest of correlated evolution requires dedicated methods. Ignoring the phylogeny results in biases when simple counting methods are applied to species traits. We illustrate this phenomenon, sometimes termed “phylogenetic inertia” [Harvey and Pagel, 1991], with a correlation test.

We must first acknowledge the history partially shared by species, that is classically represented by a phylogenetic tree. We will, therefore, account for the phylogenetic relationships between the species by modelling the evolution of traits along the tree. The most simple model of continuous trait evolution was introduced by Felsenstein [1973]. Under this model, a trait Y mutation is only described by its intrinsic variance σ_Y^2 . The evolution of the trait is modelled as a Brownian motion: the distribution $D_Y(t)$ of the evolved trait after a certain time t is a normal distribution with mean y_0 (trait at time 0) and a variance equal to $\sigma_Y^2 \times t$. To simulate the evolution of a trait along a tree, we can apply this procedure recursively on each branch of the tree, propagating the trait values down the tree. We note y_i the (ancestral) traits at node i in the tree; y_0 is the ancestral trait state at the root (node 0) of the tree. We further note the branch lengths $\{t_i\}_{1 < i < n}$ between a node i and its parent p in a rooted tree with n branches. Starting from the root of the tree, a value for each descendant node i is then drawn randomly from the distribution

$$D_Y(t_i) = \mathcal{N}(y_p, \sigma_Y^2 \times t_i), \quad (1)$$

where y_p is the value of the trait at the parent node. Figure 2 shows an example of three traits simulated with Brownian motions with distinct intrinsic variances.

Traits can be then measured at the leaves of the tree, representing a sample of species with partially shared histories. Once the traits are measured in the different species, one can compute simple correlations between the trait values.

Here we have chosen the Kendall’s τ test because it is a non-parametric rank correlation test between two numerical variables, without any assumption regarding the distribution of the data. Like most correlation tests, it considers each pair of trait values (*i.e.* a species) as an independent sampling. Under the null hypothesis of independence, if one draw randomly one set of pairs of values that have two independent distributions and compute their correlation, one has 5% chances to obtain a P value below 0.05. More generally, if one computes the distribution of P values over many such samples, we obtain a uniform distribution over $[0, 1]$.

When simulating two independent traits along the same phylogeny and assessing their correlation, we observe that the distribution of P values is skewed toward small values (Figure 4). This means that the two traits appear intrinsically correlated, despite being independently simulated along the phylogeny.

This implies that the correlation between two traits in a sample of species is the sum of an intrinsic correlation and a phylogenetic correlation. As a consequence, there is a need for methods that specifically test for the significance of the intrinsic correlation, eliminating for the phylogenetic one. One possibility is to only sample species that are very distant and/or have emerged from a rapid radiation and exhibit a star-like phylogeny. Another is to specifically incorporate the phylogeny in the method.

2.2 The phylogenetically independent contrasts

Using properties of the Brownian motion, Felsenstein [1985] introduced one of the first comparative method for continuous traits, named the phylogenetic independent contrasts (PIC). The idea behind the contrasts method is a transformation of the input variables, so that the values of each transformed variable become statistically independent. Considering a given phylogenetic tree, it occurs that the evolution of a trait y along two branches leading to a pair of node siblings i and j (e.g. 1 and 2) sharing the same parent node k (e.g. 8) is independent. As a result, the differences $y_1 - y_2$, $y_4 - y_5$, $y_6 - y_7$, $y_8 - y_3$, $y_{10} - y_{11}$ and $y_9 - y_{12}$ are all statistically independent (Figure 3). Following this logic it is possible to transform a vector of n trait values $\{y_i\}_{1 \leq i \leq n}$ into $n - 1$ phylogenetically independent contrasts $\gamma_{ij} = y_i - y_j$.

Assuming a Brownian motion, the expectation and variance of the contrasts are:

$$E(\gamma_{ij}) = 0 \tag{2}$$

$$V(\gamma_{ij}) = \sigma_Y^2 \cdot (t_i + t_j). \tag{3}$$

To compute contrasts at internal nodes, we need to reconstruct ancestral trait states. The ancestral trait value y_k for any ancestral node k with two daughter branches i and j is obtained by taking the weighted mean of the trait values at the direct descendant nodes:

$$y_k = \frac{\frac{1}{t_i}y_i - \frac{1}{t_j}y_j}{\frac{1}{t_i} + \frac{1}{t_j}}. \quad (4)$$

We can therefore compute all contrasts and ancestral traits recursively along the tree, collapsing nodes after computing their associated contrasts. For instance, using the tree depicted on Figure 3, one computes first $\gamma_8 = y_1 - y_2$ and $y_8 = (t_1^{-1}y_1 - t_2^{-1}y_2) / (t_1^{-1} + t_2^{-1})$ and then removes leaves 1 and 2. Branch length t_8 is then updated in order to accommodate the fact that y_8 was estimated and not observed, and has an additional estimation variance. This is equivalent to an additional time for y_8 to have evolved from y_9 , which depends on branch lengths t_1 and t_2 [Felsenstein, 1985]:

$$t'_8 = t_8 + \frac{t_1 \cdot t_2}{t_1 + t_2}. \quad (5)$$

y_8 and t'_8 are then used to compute γ_9 and y_9 , using formula 4.

A simple method to test for the correlation between two continuous traits while accounting for the species phylogeny consists in first transforming each variable into independent contrasts, before testing for a correlation using standard classical tests. Figure 4 shows that this method successfully removes the phylogenetic correlation, at least when the true phylogeny is known and when the underlying trait evolves under a Brownian motion.

2.3 Extending the linear model to account for phylogeny

The phylogenetic independent contrasts offer a simple way to compare different species traits. It proves, however, to be limited when testing hypotheses about trait evolution and environment variables, which are typically unknown for the ancestral species. As a consequence, these analyses are conducted within the linear modeling framework, where a given response variable y with n values $\{y_i\}_{1 \leq i \leq n}$ is modeled as a linear combination of m explanatory variables $\{x_j\}_{1 \leq j \leq m}$ with corresponding values $\{x_{ji}\}_{1 \leq j \leq m, 1 \leq i \leq n}$:

$$y_i = \hat{y}_i + \epsilon_i \quad (6)$$

$$\hat{y}_i = a_0 + \sum_{j=1}^m a_j x_{j,i}, \quad (7)$$

where a_0 is a constant (aka intercept) and the $\{a_j\}_{1 \leq j \leq m}$ are the model coefficients. The $\{x_{ji}\}$ terms may denote observed variables or some of their interactions. For two measured traits, there can be up to three possible variables (the two traits and their pairwise interaction), for three measured traits, there can be up to seven variables (the three observed traits, three possible pairwise interactions, and one triple interaction), etc. In a typical evolutionary comparative analysis, y would be a biological trait of interest (*e.g.* body mass, age of sexual maturity, sexual dimorphism, etc) and the x_j variables are either other biological variables such as life history traits, and/or environmental factors such as temperature, amount of precipitation, etc.

In the linear modeling framework, the model parameters $\{a_j\}$ are estimated using a maximum likelihood approach. The Gauss-Markov theorem states that, if the error terms $\{\epsilon_i\}_{1 \leq i \leq n}$ are uncorrelated and with identical variance (homoscedasticity), the best unbiased linear estimators are the ordinary least square (OLS) estimators, that is, the values of $\{a_j\}$ for which $\sum_{i=1}^n (y_i - \hat{y}_i)^2 = \sum_{i=1}^n \epsilon_i^2$ is minimal. Noting $Y = (y_i)_{1 \leq i \leq n}$ as the response vector and $X = (x_{i,j})_{1 \leq i \leq n, 1 \leq j \leq m}$ the data matrix, such as

$$X = \begin{pmatrix} 1 & x_{1,1} & \cdots & x_{1,j} & \cdots & x_{1,m} \\ \vdots & \vdots & \cdots & \vdots & \cdots & \vdots \\ 1 & x_{i,1} & \cdots & x_{i,j} & \cdots & x_{i,m} \\ \vdots & \vdots & \cdots & \vdots & \cdots & \vdots \\ 1 & x_{n,1} & \cdots & x_{n,j} & \cdots & x_{n,m} \end{pmatrix}, \quad (8)$$

and $A = (a_j)_{0 \leq j \leq m}$, the OLS estimator \hat{A} is obtained by the formula

$$\hat{A}_{OLS} = (X^T X)^{-1} X^T Y, \quad (9)$$

where X^T is the transposed matrix of X . If the error terms are, in addition, normally distributed, then the OLS estimators are also the maximum likelihood estimators.

The generalized linear model (GLM) framework extends the OLS estimates to a full class of models where the error terms follow distributions from the exponential family (Figure 5). The GLM framework also includes heteroscedastic models, where the variance of the error term is not uniform. A strong assumption, however, remains: that the error terms are uncorrelated, which is at odds with the tree-based history of the biological data.

Another extension, the generalised least square (GLS) framework, integrates a correlation structure into the ordinary least square estimators. Basically, it

includes a variance-covariance matrix of individuals in the trait space, noted V . V is a square matrix of size n , the sample size. The GLS estimates of A are then simply given by the formula

$$\hat{A}_{GLS} = (X^T V^{-1} X)^{-1} X^T V^{-1} Y. \quad (10)$$

An interesting property of the GLS procedure is that the variance-covariance matrix, V , does not need to be fully specified, and free parameters can be estimated jointly with the regression coefficients within the maximum likelihood framework.

Assuming a Brownian motion to model the evolution of continuous traits, the matrix of variances and covariances between species can be obtained directly from the branch lengths of the corresponding phylogenetic tree (Figure 6): the variance for each species is given by the total branch lengths from the root of the tree, while the covariance between two species is equal to the total length between the root and the most recent common ancestor of the two species. Grafen [1989] was the first to propose the use of a GLS procedure as a way to account for phylogeny in the comparative analysis. The method was later extended by Martins [1994] and Martins and Hansen [1997] and re-branded as ‘‘Phylogenetic Generalized Least Squares’’ (PGLS). When a purely bifurcating tree is used with a Brownian motion model, the PGLS boils down to the simpler PIC method [Felsenstein, 2003]. Paradis and Claude [2002] later further extended the framework using generalized estimating equations (GEE, Figure 5). A powerful property of the GLS and GEE frameworks is the possibility to test different models of evolution along a phylogeny, beyond the simple Brownian motion. Blomberg et al. [2003], for instance, extended the original Brownian motion to include heterogeneity in the rate of evolution.

Regardless of the model, there is a need for a phylogeny with estimated branch lengths. It is typically obtained from a different source, for instance molecular sequences. In many cases, the resulting branch lengths, which depict the evolutionary rates of particular genes, have *a priori* little to do with the evolution of the trait under study. Branch lengths, however, cannot be estimated from the trait data as this would result in too many free parameters. Grafen [1989] proposed a method to compute branch lengths for a given topology with a single parameter ρ . While the ρ parameter does not have a particular biological interpretation, it adjusts the amount of treelike evolution: while $\rho = 0$ results in all internal branches to be equal to 0, effectively turning the phylogeny into a star tree with null covariances, $\rho = 1$ reduces all terminal branches to 0 and the data to simply two points. Estimating ρ together with the regression parameters

thus offers a way to quantify the amount of phylogenetic correlation in the data, and to account for it when testing other effects. Finally, Martins and Hansen [1997] departed from the Brownian motion and considered a model where the covariance between two taxa depends on their phylogenetic distance t_{ij} :

$$V_{ij} = \gamma \exp(-\alpha \cdot t_{ij}). \quad (11)$$

The matrix V corresponding to the tree in figure 6 is:

$$V_{Martins} = \gamma \exp \left[-\alpha \begin{pmatrix} 0 & l_{1,2} & l_{1,6,3} & l_{1,6,7,8,4} & l_{1,6,7,8,5} \\ l_{2,1} & 0 & l_{2,6,3} & l_{2,6,7,8,4} & l_{2,6,7,8,5} \\ l_{3,6,1} & l_{3,6,2} & 0 & l_{3,7,8,4} & l_{3,7,8,5} \\ l_{4,8,7,6,1} & l_{4,8,7,6,2} & l_{4,8,7,3} & 0 & l_{4,5} \\ l_{5,8,7,6,1} & l_{5,8,7,6,2} & l_{5,8,7,3} & l_{5,4} & 0 \end{pmatrix} \right] \quad (12)$$

where $l_{x,y,z,\dots} = l_x + l_y + l_z + l_{\dots}$ and $\exp[M]$ denotes the element-wise exponential of a matrix M . The coefficients α and γ can be interpreted in terms of constraining force and inter-specific variance of a model of stabilizing selection [Martins and Hansen, 1997].

2.4 Correlation between discrete traits

Although methods for correlated evolution of discrete traits can be studied by the linear model framework, discrete traits coevolution has been the subject of specific developments. Building on the methodology of maximum parsimony, the transitions between trait states can be inferred and mapped on the branches of a phylogeny. In its simplest form, one first reconstructs the ancestral states at all internal nodes, and then counts one transition event on each branch where the states at the ancestral and descendant nodes are different (we will see a more advanced approach in section 3.2). For a single binary trait with two states 0 and 1, there are two possible transitions: $0 \rightarrow 1$, and $1 \rightarrow 0$. For a pair of binary traits, there are four possible pairs of states, 00, 01, 10, and 11 and twelve possible transitions. Ridley [1983] built a contingency table by counting the number of occurrences of each combination of traits at the end of branches where at least one trait had undergone a transition. As mutations on different branches of the tree can be considered independent, one can test independence using standard tests (χ^2 or Fisher's exact test).

The method of Ridley [1983] tests for covariation of traits, regardless the direction of mutation. It does not distinguish whether mutations in the first trait tend to cause mutations in the second. Such information can be inferred from

branches where only one of the two traits undergoes a transition, noting the state of the other trait. Maddison [1990] introduced a method where one of the two traits is treated as a conditional variable, and assessed whether the transitions at the other trait are distributed randomly according to the conditioned trait along the phylogeny.

Harvey and Pagel [1991] extended the methods of Ridley [1983] and Maddison [1990] using a continuous time Markov model of trait evolution to compute the likelihood of the species distribution of states, given the underlying phylogeny. For binary traits, the generator of the Markov model is

$$Q = \begin{pmatrix} -q_{0 \rightarrow 1} & q_{0 \rightarrow 1} \\ q_{1 \rightarrow 0} & -q_{1 \rightarrow 0} \end{pmatrix}, \quad (13)$$

where $q_{x \rightarrow y}$ denotes the rate of transition from state x to state y . This model is conceptually similar to the one introduced by Felsenstein [1981] for modeling sequence evolution, from which it borrows the so-called pruning algorithm (dynamic programming) to efficiently integrate over all possible ancestral states.

One can then properly compute a likelihood for the mutations in the tree. The likelihood function can be maximised to estimate the transition matrix. Interestingly, Harvey and Pagel [1991] used this likelihood framework to compute the mean number of mutations on each branch of the phylogeny for each trait independently. A correlation coefficient can subsequently be computed to assess the independence between the evolution of the two traits.

This approach was further extended by Pagel [1994], who considered pairs of trait states in the Markov chain: 4 combined states and at most 12 transitions. More specifically, he used the following generator to model the correlated evolution of both traits:

$$Q_{\text{pair}} = \begin{pmatrix} -q_{00 \rightarrow 01} - q_{00 \rightarrow 10} & q_{00 \rightarrow 01} & q_{00 \rightarrow 10} & 0 \\ q_{01 \rightarrow 00} & -q_{01 \rightarrow 00} - q_{01 \rightarrow 11} & 0 & q_{01 \rightarrow 11} \\ q_{10 \rightarrow 00} & 0 & -q_{10 \rightarrow 00} - q_{10 \rightarrow 11} & q_{10 \rightarrow 11} \\ 0 & q_{11 \rightarrow 01} & q_{11 \rightarrow 10} & -q_{11 \rightarrow 01} - q_{11 \rightarrow 10} \end{pmatrix} \quad (14)$$

further assuming that the two traits cannot mutate simultaneously and thus reducing the transition matrix to 8 parameters. When the two traits are independent, the transition matrix can be even further simplify to 4 parameters, two transitions for each trait. [Pagel, 1994] then suggested to compare the likelihood maximized over the 4 or 8 parameters (resp. \mathcal{L}_{4p}^{\max} and \mathcal{L}_{8p}^{\max}). As both models are nested –the 4 parameter model is defined in a sub-space of the general one–, we can test whether the likelihood increase due to the extra parameters

is significant. A model with more parameters always fits better, and the use of likelihood ratio tests is standard to compare nested models: under independence, the quantity $2(\ln \mathcal{L}_{8p}^{\max} - \ln \mathcal{L}_{4p}^{\max})$ converges to a χ^2 distribution with 4 degrees of freedom. The generality of this framework permits to test various hypotheses about the evolutionary process, including the order of mutations along the phylogeny. The relatively large number of parameters involved, however, restricts its application to relatively large data sets.

2.5 Examples of correlated traits

Applications of phylogenetic comparative analysis fall within two categories: (i) inferring the factors that drive the evolution of one or several traits, and (ii) assessing the correlated evolution between several traits. One of the most studied trait is the body mass index, which correlates with many other physiological and environmental variables [Cooper and Purvis, 2010]. It was mostly studied in mammals, for which large data sets are available, as well as a well-studied phylogeny. These studies revealed an important historical component [Gittleman, 1985, Cheverud et al., 1985], but also geographical and environmental factors such as temperature, altitude and species richness [Cooper and Purvis, 2010]. Paradis and Claude [2002] used GEEs to reassess the relationship between species dispersal and population synchrony (defined as the correlation of population size variations between localities [Lande et al., 1999]). It accounts for dispersal, habitat and the interaction of the two factors, together with a long term effect (time series) and the underlying phylogeny of the species. Their model confirms the existence of an habitat-specific effect of dispersal, but shows that the long term effect vanishes when phylogeny is properly accounted for.

Other studies used phylogenetic comparative analysis to assess correlated evolution between distinct traits. An example of such correlated traits is the average vs. sex dimorphism in species body mass. The “Rensch rule” [Rensch, 1950] stipulates that sexual dimorphism increases with the average body mass in species where the male is the largest, while it decreases in species where the female is larger than the male [Fairbairn, 1997]. Abouheif and Fairbairn [1997] used phylogenetic independent contrasts to put this rule at test with 21 animal taxa. They found that, besides one single exception, allometric relationships follow the pattern of Rensch rule. Lenormand and Dutheil [2005] looked at another sexual dimorphism, the difference of recombination rate between females and males (heterochiasmy). They fitted a GEE model to a plant data set and assessed the factors driving the evolution of heterochiasmy. There, the trait

under study was the ratio of sex-specific average recombination rate, and the explanatory variables included, in addition to the phylogeny of the species, the presence of sex chromosomes and the selfing rate. This model allowed the authors to test the Haldane-Huxley hypothesis, which stipulates that in species where recombination is suppressed in one sex, this sex is always the heterogametic one. The pattern, however, does not hold for so-called heterochiasmate species, where both sexes recombine but at a distinct rate. Lenormand and Dutheil [2005] showed that the presence of sex chromosomes had no significant effect on the difference of recombination rate between sexes, but that the selfing rate did, as predicted by a model with differential selection during the haploid phase [Lenormand, 2003].

2.6 Jointly modeling traits and sequences

An interesting complementary approach tested for correlated evolution between transition rates of molecular evolution and several morphological traits [Lartillot and Poujol, 2011]. Rates of molecular evolution, such as dN , the rate of amino-acid changes (non-synonymous) or dS , the rate of synonymous mutation rate, are modeled as continuous traits. Although one can only hardly measure rates, even at the leaf of the tree, the sequences at the leaves of the trees are informative on the mutation processes. The mutational rates are modeled explicitly, as in classical phylogeny, but their rates vary as a Brownian motion, whereas they are held constant in standard phylogeny. The ambition of such models is to find morphological traits, or life history traits, that strongly correlate with molecular rates variation. Lartillot and Poujol [2011] found that body mass and longevity positively correlate with the intensity of selection, proxied by the ratio dN/dS . The same framework was also used to explore the interplay between biased gene conversion, selection and other traits [Lartillot, 2013]. Finally, it was also used to explore how the variation of mutation rates and their correlation to traits could bias the inference of the phylogenetic tree itself [Lartillot and Delsuc, 2012].

3 Correlated evolution within genomes

Genetic sequences can be viewed as traits with simple, well-defined discrete states (4 states for each site). Unlike morphological traits, the mechanisms of their evolution are well understood, with explicit models of transitions along a phylogeny. As a result, increasingly complex models of sequence evolution

have been developed [Yang, 2006]. Correlated evolution of the molecular traits can thus be investigated using statistical methods that are similar to the ones described in section 1 for morphological traits. The current section presents different approaches that have been conducted, classified according to the selection level that they consider, from single nucleotides to complete genomes.

3.1 Within genes, between nucleotides

One can trace back the study of intra-molecular coevolution to the research on RNA molecules. When Holley et al. [1965] sequenced the first transfer RNA (tRNA) molecule, they proposed three possible structures based on the occurrence of stretches of Watson-Crick pairs, forming putative double helices. When a second tRNA sequences was obtained, the only common possible structure was one with a “cloverleaf” shape, which was then proved to be common to all tRNAs [Westhof and Auffinger, 2012]. This conservation of tRNA structure opened the way to comparative sequence analysis as a way to extract information regarding evolutionary constraints and, ultimately, biological functionality – as envisioned by Crick [Cobb, 2017].

The Watson-Crick base-pairing, that associates A-U and G-C, leads to an important evolutionary prediction: if two positions in a RNA molecule are interacting to form a Watson-Crick pair within a double helix, the paired nucleotides with states A-U, U-A, G-C and C-G have a similar fitness and are thus interchangeable. Conversely, any of the other pairs leads to a structural instability and, therefore, a lower fitness. Consequently, when comparing multiple homologous paired positions in different genes, we expect a high frequency of A-U, U-A, G-C and C-G, and a low frequency, if any, of the other combinations. This results in a two-site fitness landscape where Watson-Crick pairs are “peaks” connected by two mutation events, one at each site, as illustrated in Figure 1D [Dutheil et al., 2010]. A resulting property of this landscape is that the fitness effect of a mutation at one site (and consequently, its probability of fixation) depends on the state at the interacting site. Such epistatic interactions result in a scenario of coevolution by compensation: a deleterious mutation can be compensated by another mutation at an interacting site, and the evolution of the two positions become correlated. This reasoning served as a basis for many molecular coevolution studies. Identifying correlated evolution within a gene tells something about the structural and functional constraints of the encoded molecule.

This principle was first applied to the prediction of RNA structures, given

the clear expectation of coevolution at sites located within double-stranded helices (see <http://www.rna.icmb.utexas.edu/CAR/> for a historical perspective). The comparative analysis of RNA sequences starts with a multiple sequence alignment. The most simple approaches initially counted the number of Watson-Crick pair occurrences in all pairs of alignment columns, while subsequently developed approaches used more elaborated statistical methods. One of the earliest but still popular method uses the so-called mutual information (MI) measure, defined as the sum of the Shannon entropy of the two positions, minus the joint entropy of the pair [Chiu and Kolodziejczak, 1991]:

$$\begin{aligned}
 MI(x, y) = & - \sum_i f(x_i) \log(f(x_i)) \\
 & - \sum_j f(y_j) \log(f(y_j)) \\
 & + \sum_i \sum_j f(x_i y_j) \log(f(x_i y_j)) \quad (15)
 \end{aligned}$$

where x and y are two columns in the alignments. $f(x_i)$ and $f(y_j)$ denote the frequencies of each nucleotide i at site x and each nucleotide j at site y , respectively. Besides, $f(x_i y_j)$ denotes the frequency of each pair of nucleotides i and j at the two sites. Given that $\sum_i f(x_i) = 1$ and $\sum_j f(y_j) = 1$, we have $\sum_i f(x_i y_j) = f(y_j)$ and $\sum_j f(x_i y_j) = f(x_i)$. Equation 15 can then be factorized and reorganized in:

$$MI(x, y) = \sum_i \sum_j f(x_i y_j) \log \left(\frac{f(x_i y_j)}{f(x_i) \times f(y_j)} \right). \quad (16)$$

If the two positions x and y are evolving independently, then $f(x_i y_j) = f(x_i) \times f(y_j)$, and $MI(x, y) = 0$. A MI value departing from 0 is therefore a signature of non-independent evolution.

A difficulty arises, however, when trying to evaluate the significance of $MI(x, y)$ as sequences partially shares history (again represented by a phylogeny). Consequently, MI values will generally be positive for most pairs of sites [Dutheil, 2012] and properly assessing the null distribution of MI values requires accounting for the phylogeny. This can be achieved by correcting the $MI(x, y)$ value using information from the full sequence alignment (assuming coevolving pairs are a minority among all possible pairs) or by simulations (see Dutheil [2012] for a review).

While it is possible to properly account for the evolutionary history of the species when computing the null-distribution of the MI statistics, this statistics is based on the sequence patterns only and is intrinsically agnostic of the

underlying evolutionary paths. Several authors, therefore, designed models of coevolving positions, related to the model introduced by Pagel [1994] (see section 1), restricted to pairs of sites to avoid an excessively large number of parameters. For nucleotides, the model has 16 states and at most 240 transitions (but as for the original model of Pagel, the number of transitions can be reduced by banning double mutations and by imposing constraints on the reversibility of transitions). Tillier and Collins [1995, 1998] were the first to design a nucleotide model, which they applied to ribosomal sequences. A convenient aspect of this framework is that it is straightforward to derive the expected model when both sites evolve independently. This independence model can be used as a null-model and compared to the correlated model, using for example likelihood ratio tests. It requires, however, to fit a model for all pairs of sites, which can be relatively resource demanding. Yeang et al. [2007] used a similar model, which they combined with a hidden Markov chain along the alignment in order to capture spatial dependencies, for instance within secondary structure motifs. Finally, Dib et al. [2014] used a general Pagel model, and employed a Bayesian inference procedure in order to jointly estimate model parameters, but also the coevolutionary “profile” of coevolving states among possible state pairs, as well as the underlying phylogeny [Meyer et al., 2019]. Such approaches, combining sophisticated statistical inference and efficient computational implementations are very powerful tools to study coevolutionary processes within sequences.

3.2 Within proteins, between amino-acids

Characterizing correlated evolution within proteins is intrinsically more challenging, because of the larger number of states. While the 20 amino-acid lead to a putative 400 possible pairs of states for two coevolving positions, all these combinations may not differ in their fitness. Because the 20 amino-acids have redundant biochemical properties, some may be interchangeable at some positions in the protein without any notable fitness effect.

The year 1994 was particularly important for the study of protein coevolution. Shindyalov et al. [1994] introduced a new probabilistic method that “mapped” substitutions on the branches of a phylogenetic tree in order to assess how likely two positions are to undergo substitutions on the same branches of the tree, if they were evolving independently. Shindyalov et al. [1994], Göbel et al. [1994] then asked how the three-dimensional structure of proteins impacts the occurrence of coevolution; in particular, whether residues in contact in the tertiary structure tend to have a correlated evolution. Neher [1994] developed

a different statistical framework to address the same question. While his approach does not account for the underlying phylogeny, it proposes an attempt to account for the biochemical properties of proteins. By weighting each amino-acid by a given biochemical index, he assessed how correlated are biochemical properties between sites in a protein.

Pollock et al. [1999] used an approach similar to that employed by Tillier and Collins [1998] to model the correlated evolution of RNA sites, but for proteins. In order to reduce the complexity of the model, which would contain a total of 400 states, they grouped several amino-acids according to their biochemical properties. If two categories are considered (for instance “large” and “small” residues), the model only has four states (large-large, large-small, small-large, small-small) to account for. It is similar to the general model introduced by Pagel [1994], yet the authors lowered the number of parameters (by making the model reversible).

Tufféry and Darlu [2000] introduced an intermediate approach. Building on Shindyalov et al. [1994]’s work, they first used a phylogeny to reconstruct the ancestral sequences at all inner nodes in the tree, and inferred on which branch and site substitutions occurred. They then evaluated which positions in the alignment tended to undergo substitutions on the same branches of the tree, introducing the term *co-substitution* to denote branches with mutations at both sites. Dutheil et al. [2005] and [Dutheil and Galtier, 2007] later extended this method to account for the branch lengths of the tree and the uncertainty of the ancestral states, a procedure called *substitution mapping*. They further introduced the possibility to include biochemical weights, following Neher [1994]. A complementary development considers not only co-substitutions, but also sequentially ordered events (see Figure 7d), where substitutions at one site (the leading events) trigger substitutions at another site (the lagging events) [Kryazhinskiy et al., 2011, Behdenna et al., 2016]. Once mutation events are placed on the tree, it is possible to compute analytically the probabilities under independence of any type of pairs (co-substitutions, ordered pairs, exclusive pairs, etc.) [Behdenna et al., 2016]. Such semi-parametric approaches are more efficient than full-model based approaches as they do not explicitly model site dependence. Yet the underlying models account for many aspects of the evolutionary process, and can be applied to both nucleic acids and proteins [Dutheil et al., 2005].

Parallel to the development of phylogenetically grounded methods, methods solely based on the alignment have recently shown spectacular development. A popular and successful approach is to fit a generalized Ising model (Potts model)

into the alignment of L amino-acid sequences, disregarding the phylogeny. Ising models consist of discrete variables that represent atomic "spins" that can be in one of two states (+1 or -1). The spins are arranged in a graph, usually a lattice, allowing each spin to interact with its neighbors (pairwise interactions). Generally, neighbors spins are only compatible when of the same sign. One can then compute the probability of the whole graph to be in a configuration using marginal probabilities of each spin and pairwise interactions between them. The Potts model allows for more than two states (not only +1/-1). These models, developed in statistical physics, take into account local abundances and pairwise interactions, but disregard higher order interactions. DCA (Direct Coupling Analysis) [Weigt et al., 2009, Morcos et al., 2011] is a successful implementation of a method based on this model.

The Potts model assumes that each sequence of the alignment has a probability of being sampled that is given by a Boltzmann-like distribution. The higher the probability, the more abundant is the sequence in nature. Low probability sequences correspond to deleterious combinations of the amino-acids that one should not encounter in nature. A sequence $a_1 a_2 \cdots a_n$ has a probability $P(a_1 a_2 \cdots a_L) = \frac{1}{Z} \exp(-\mathcal{H}_{a_1 a_2 \cdots a_L})$ of being observed. Z is a normalisation constant, equal to the integral of $\exp(-\mathcal{H})$ over the whole sequence space. The "Hamiltonian" function \mathcal{H} has both a local abundance component h and a pairwise epistatic component e . More precisely, it is computed as:

$$\mathcal{H}_{a_1 a_2 \cdots a_L} = \sum_{i=1}^L h_i(a_i) + \sum_{i=1}^L \sum_{j=i+1}^L e_{ij}(a_i, a_j)$$

The sums are taken over all positions of the alignment. In this formulation, the function h takes $21 \times L$ input variables (gap is a 21st symbol) and returns a quantity related to the marginal probability of observing one of the 21 symbols at position i . The e function takes $(21 \times L)^2$ input variables and returns a quantity related to the symmetrical interaction between amino-acids (and gaps) for each pair of positions i, j , with $e_{ij}(a, b) = e_{ji}(b, a)$ and $e_{ii}(a, b) = 0$.

One reason proposed to justify the Potts model for protein sequences is that the correlation observed between two columns in an alignment is not a good indicator of a direct functional or structural interactions. In the case of structure for instance, a correlation can be the result of a contact between two residues (a true signal of correlated evolution), but can also reflect indirect interactions: e.g. a_i and a_j are distant in the structure, but close to a third residue a_k , then resulting in indirect interactions. In the Potts model, the probability distribution only considers direct coupling effects. The hope is that

those couplings reflect biologically relevant interactions. In this regard, only the e function is important.

In the end, the difficulty comes when the functions h and e must be inferred from the data, a challenge named the *inverse Potts problem*. Several techniques were proposed, from simple moment estimations to maximisation of the \mathcal{H} function in its gigantic parameter space [Weigt et al., 2009, Morcos et al., 2011, Baldassi et al., 2014, Ekeberg et al., 2013]. The method performs especially well, when a very large number of “pseudo-independent” sequences are provided in the alignment. Indeed, it is noteworthy to mention that, to correct for the phylogenetic inertia, closely related sequences (by default with $> 70\%$ of identity) are grouped into clusters and each member of the cluster has a weight inversely proportional to the cluster size. This also corrects for bias sampling of the protein families in the database, as some clades are typically over-represented (e.g. vertebrates). DCA was originally developed to predict structural contacts between amino-acids [Weigt et al., 2009], but as also used to find contacts in RNA [De Leonardis et al., 2015] or predict the effect of mutations on a query sequence [Figliuzzi et al., 2016].

While most methods typically exploit either evolutionary paths in phylogenies or counts in the alignment, others searched a compromise between the two, with the explicit goal to maximise the input information while keeping the computation time low. In CAPS [Fares and Travers, 2006], the authors designed a score for two sites that uses all pairwise comparisons of the sequences; it thus takes into account the pairwise distances matrix between the sequences but does not reconstruct a tree. In the BIS method [Dib and Carbone, 2012] and BIS2 [Champeimont et al., 2016], subsequent residues that show strong patterns of co-abundance are first merged into blocks. All pairs of blocks are then tested for co-evolution by computing a metric of co-abundance in the alignment (an MI-like score). The metric is finally recursively re-weighted by the co-abundances in all subtrees, starting with the root node (the root node encompasses all sequences). Consequently, the topology of the tree (not the branch lengths) is incorporated in the metric. Finally more recently, persistence time in the phylogeny of co-conservations (not co-variations) for a pair of sites has been suggested to be a good sign of co-evolving positions [Laine et al., 2019].

Residues showing strong patterns of correlated evolution are typically in contact in the 3D structure of the folded protein [Pollock et al., 1999]. It is noteworthy to mention that coevolving residues detected by methods geared to direct coupling such as DCA-like are typically closer in space than methods solely based on correlation of abundances in the alignment, such as MI-like

[Marks et al., 2011]. Conversely, it has been proposed to use the graph of co-evolving residues to guide the folding of peptides, a major challenge of structural biology. Recently developed folding methods, such as in the EVfold suite, use the predictions of DCA to greatly improve the folding accuracy [Marks et al., 2011, Hopf et al., 2012].

The continuous development of innovative methods to study patterns of co-variation in biological sequences has led to a better understanding of the relation between coevolution of sites and their functional linkage. Yet, several theoretical aspects of sequence coevolution remains poorly understood. What are the mechanisms by which co-substitutions occur? What is the role of compensatory mutations in sequence coevolution? What is the connection between coevolution and the rate of evolution at single sites? Answering these questions requires input from related fields of study, such as empirical fitness assessment [Visser and Krug, 2014], experimental evolution [Long et al., 2015], as well as modeling [Talavera et al., 2015].

3.3 Within genomes, between genes

Cellular functions are the results of multiple protein interactions. Many proteins interact with more than one partner, resulting in a network of protein interactions. As proteins involved in the same network are likely to share some selective constraints, they are expected to coevolve, similarly to sites within individual proteins. Inferring the interaction partners of a protein is of great interest to elucidate the functional role of a candidate gene. Therefore, several studies aimed at inferring correlated evolution to predict protein-protein interactions [de Juan et al., 2013].

A pioneering method, known as *mirror-tree* detects genes with similar phylogenetic trees [Goh et al., 2000, Pazos and Valencia, 2001]. In its early implementation, the method simply looks at the correlation between distance matrices computed from two protein sequence alignments: because of common evolutionary constraints of interacting proteins, their rate of evolution will be correlated as they adapt simultaneously to the changing environment and, therefore, accumulate substitutions in the same branches of the tree. These assumptions are “co-departures from a clockwise evolution” [Galtier and Dutheil, 2007]. Yet, neutrally evolving proteins, which evolve under a molecular clock, will show a strong correlation of their genetic distances as they share a common history of speciation events. Accounting for this common phylogenetic context has been the focus of later developments [de Juan et al., 2013].

With the advent of genome sequencing, exhaustive information regarding the proteome content of species became available. This allowed the reconstruction of *phylogenetic profiles* (= *phyletic patterns*), defined as the patterns of presence/absence of homologous genes in a set of species. Barker and Pagel [2005] applied the method of Pagel [1994] (see Section 2.4) to phyletic patterns from more than 10,000 protein pairs in order to detect linked genes. Using a set of known interacting proteins from *Saccharomyces cerevisiae*, they found that functionally interacting pairs indeed show a signal of coevolution, and that using phylogeny-aware coevolution detection methods significantly improves the prediction of functional interactions. The “discrete coevolution” model, however, requires several transition parameters to be estimated for each tested pair of proteins. Barker et al. [2007] later showed that fixing some of these parameters further improves the predictions.

An alternative approach originates from the studies of the rates of genes gains and losses. These studies summarize the patterns of presence-absence of many gene families into a large matrix of 0 and 1, with species as rows and genes as columns, similar to a sequence alignment. Using the model introduced by Harvey and Pagel [1991] for single binary characters, it is possible to infer rates of gains and losses by maximum likelihood. In this approach, the number of parameters to estimate is considerably reduced, as they are shared by all genes, which resolves some of the estimation issues when fitting the same model on each gene independently. Yet, it also makes unrealistic assumptions, as some gene families are known to undergo higher rates of gene gains and losses than others. To accommodate this issue, Cohen et al. [2008] proposed a mixture model allowing for these rate parameters to follow an *a priori* distribution and, therefore, to vary between genes while introducing only a few additional parameters. Applying the substitution mapping approach introduced for mapping nucleotide and amino-acid substitutions [Dutheil et al., 2005] to the presence-absence model, Cohen et al. [2012] inferred events of co-gain and co-losses along the phylogeny to infer co-evolving genes. Using simulations, they show that this approach largely outperforms simpler methods based on the correlation of patterns only. The authors also showed that it gave slightly better performances than the Barker and Pagel [2005] model, with less than 1% of the computational time, owing to the lower number of parameters to estimate [Cohen et al., 2013].

Finally, it is worth mentioning that the physical interaction between proteins involves biochemical mechanisms acting at the amino-acid level. As a matter of fact, DCA was first developed to predict contact residues between two peptides [Weigt et al., 2009] and then improved to detect contact residues between

two proteins [Szurmant and Weigt, 2018]. Conversely, DCA outcomes can be used to predict how two domains interact [Hopf et al., 2012]. However, finding co-evolving sites between pairs of proteins greatly increase the computational load, $n_1 \times n_2$ comparisons have to be assessed between two genes encoding n_1 and n_2 amino-acids, respectively. Therefore, few methods were subsequently developed to apply a DCA-like strategy at the scale of complete genomes, such as superDCA [Puranen et al., 2018]. Obviously, MI based methods can also be used to search for interacting partners of proteins [Bitbol, 2018], overcoming the computational cost of the inverse Potts problem. Recently, an efficient implementation of MI was used to scan interactions between all pairs of nucleotides in alignments of complete bacterial genomes [Pensar et al., 2019].

Finally, it worth mentioning that the phylogenic approach was also applied to this problem. Yeang and Haussler [2007] tackled this challenge by introducing a model of coevolution with only one additional parameter compared to the independent model. This parameter penalises simple substitutions while favoring cosubstitutions. Combining data filtering and using a computer grid, the authors could evaluate 0.1 trillion pairs of potentially interacting sites, and found that most coevolving pairs are also functionally interacting. A general issue with the detection of inter-genic correlated evolution is the assumption of a unique phylogeny shared by the two interacting genes. While phenomena like horizontal gene transfers are implicitly incorporated in models of gene gains and losses, gene duplication events are usually not, and at best, duplicated genes are discarded from further analyses. This problem remains largely unaddressed (but see Yeang [2008]), and calls for a unification of methods to detect correlated evolution with methods of tree reconciliation.

4 Genetics is also correlated evolution

In this final section, we suggest that the whole history of gene mapping, since its very beginning, can be included in the large view of correlated evolution. Genetics can be considered as a specific case of correlated evolution where the first trait is discrete –presence/absence of a variant in the genome– and the second is a phenotype of interest. Geneticists search for positive correlations between a phenotypic trait that is observed and a genetic trait that is unknown. In genetics, there is obviously a very strong support that we should interpret these correlations as causalities, where the presence of the allele in the genome ultimately causes the phenotype. Most methodologies of genetic mapping rely on exhibiting the joint occurrence (*i.e.* a correlation) of one or several alleles

with the phenotype. Our ambition is not to give a full and thorough review of the history and methods in genetics, but instead to suggest that ideas of correlated evolution may well have been growing with the rise of genetics in the early 20th century.

4.1 In individuals

After the rediscovery of Mendel work in 1900 [Moore, 2001], started the rise of gene mapping, with research programs such as the one of TH Morgan group [Morgan, 2018]. The ambition was both to isolate the factors that segregated with phenotypes of drosophilas, and then to infer the linear genetic map of these factors. The phenotypes at stake were mostly natural mutants that were easily identifiable, such as mutants in eye-coloration or wing patterns. The experimental protocol consists mainly in two steps.

First testing whether a trait would segregate according to Mendel laws (each allele has a 0.5 chance of being transmitted to a progeny) by counting the number of descendants with or without the trait of interest in a controlled mating. It is noteworthy to mention that the existence of dominant and recessive alleles in diploids, described by Mendel [1866], add a modest complication for characterizing the transmissions. One must cross an individual with a dominant trait (A/-) with an individual without (-/-) to observe 50% of the progeny harboring the phenotype. The observation that a trait would be transmitted with known and explicit rules demonstrates that a yet unknown genetic factor perfectly correlates with the presence of the trait. Interestingly the correlation between the allele and the trait is uniquely demonstrated by the observed segregating ratio.

The second part of Morgan's group work consists in controlled matings between males and females with two phenotypic traits. Using counts of co-occurrence between two traits in the progeny, they inferred the "linkage" between the corresponding genetic loci. A very simple estimation procedure of the linkage between two loci encoding two different dominant traits (say A and B) relies on counting in the progeny how many times a female¹ with both traits in linkage (an AB phenotype, corresponding to an AB/- genotype) mated with a male with no phenotype (genotype -/-) would produce progenies with 0, 1 or the 2 traits. When the original combination is kept, only descendants with 0 or 2 traits are observed. The mere observation of descendants with a single trait demonstrates the existence of new combinations of alleles that were named *recombinations*. A first estimator of the recombination probability is the observed

¹males do not recombine in drosophilas

fraction of descendants with a single trait. Consequently, recombination rate, computed as such, never exceed 0.5: traits mapped to independent loci have a 0.5 chance of being co-transmitted. The general method relied on observing correlation between traits to infer correlation between loci.

By combining the pairwise measures of recombination rate, the group showed that the loci underlying the traits were arranged linearly in what they called linkage groups. The order and the distances between the loci can be computed using pairwise recombination rates by the transformation: $d = -50 \ln(1 - 2r)$, where r is the recombination rate. These distances, named centiMorgan (cM), transform the $[0, 0.5]$ range of recombination rate to proper $[0, \infty]$ distances.

Although controlled matings were further done with almost all living organisms (including bacteria), it was not possible for humans, for obvious ethical reasons. Therefore, to map traits to loci in humans, researchers had to rely on other methods such as pedigree analysis.

4.2 In pedigrees

Pedigree analysis turned out to be a major tool in human genetics until the rise of association mapping in the 21st century. In a pedigree analysis, geneticists follow the segregation of a phenotypic trait, a pathology in medical genetics, over two, three or ideally more generations. The trait is often binary: ill or not. Pedigree analysis is mostly suited to track dominant alleles. An example of a pedigree is presented in Figure 8.

An implicit assumption of a pedigree analysis is that the phenotype is caused by an allele located at a single locus. By following the segregation of the trait, we infer the segregation of the causative allele. Using genotyping technologies, one can then genotype many loci throughout the genome for alleles that display a strong, possibly maximal, positive correlation with the phenotype. Geneticists leverage the correlated segregation between an observable phenotypic trait and a fully determined genotypic alleles to “map” a causative allele in a region of the genome. Until recently, only chosen markers distributed in genome were genotyped; consequently, the alleles co-segregating with the phenotype were not causal, but only genetically linked with an unseen causal variant located nearby. Nowadays, as complete genome sequences are available, the causal allele is among the set of alleles that co-segregate with the trait.

The most popular metrics of co-segregation is the *lod score* [Morton, 1955], a log of an odd-ratio. This odd ratio divides the likelihood of the observed co-segregation assuming linkage ($r < 0.5$) to the likelihood of the observed co-

segregation assuming independence ($r = 0.5$):

$$S_r = \log_{10} \left(\frac{\mathcal{L}_{\mathbf{P}}(r < 0.5)}{\mathcal{L}_{\mathbf{P}}(r = 0.5)} \right)$$

To compute the likelihood, one follow the line of transmission of the allele with the phenotype. For example, in figure 8, if one assumes that allele A is linked to a causal allele located at distance r , the probability of observing the genotype of individual II.1, knowing that he has the phenotype, is $(1 - r) \cdot \frac{1}{2}$: A did not recombined from the causal variant ($(1 - r)$) and he received the allele c from his mother ($\frac{1}{2}$). The genotype of individual II.2 has probability $\frac{1}{4}$. In individual III.4, there must have been a recombination between the allele A and the causal variant; the probability is then $r \cdot \frac{1}{2}$. Overall, we have:

$$\mathcal{L}_{\mathbf{P}}(r) = \frac{(1 - r)^3 r}{2^{10}}$$

More generally, the lod-score can be computed as

$$S_r = \log_{10} (2^{NR+R} \times (1 - r)^{NR} \times r^R)$$

where NR is the number of co-segregations of the focal allele with the phenotype (Non-Recombined) and R the number of recombinations. The value of r that maximizes the likelihood (and the lod-score) is the natural estimate $\hat{r}_{ML} = R/(R+NR)$. By scanning the genome for strong associations, geneticists usually identify one region containing several markers with maximal lod-scores, named a haplotype. This region contains the unseen causal variant, which requires further sequencing and functional analyzes to be confirmed. It is usually recommended to reach a lod-score of 3 to claim a strong co-segregation [Nyholt, 2000]: the odd of linkage is 1000 times times the odd of independence.

4.3 In the population

In rare cases, multiple haplotypes correlate with the phenotype. However, when the trait is not digenic but polygenic, another corpus of methodology is more suited: the association mapping. Fundamental hypotheses of association mapping stems from quantitative genetics, where traits of interest are no more binary but continuous. The apparent continuity emerges from the combination of many loci of small effects, an assumption known as the *infinitesimal model* [Barton et al., 2017].

In association mapping, instead of a family, one uses the population phenotypic diversity to find independent genetic variants that contribute to the

phenotype. For a binary phenotype, the assumption is that detected variants modulate the probability of having the phenotype, or that the pathology becomes visible only once a certain quantity of an invisible continuous trait is reached.

Association mapping at the scale of the genome is known as Genome Wide Association Study. In GWAS, geneticists measure the independent contribution of all variants segregating in a cohort to the phenotype of interest, assuming additive independent contribution for each locus. In a simple case, for a given locus l hosting two alleles A and a , a genotype \mathcal{G} is 0, 1 or 2 copies of the A allele. The statistical correlation between the number of A in the genotype and the trait is computed either by a contingency table or by linear regression.

Contingency table: for a binary trait $\mathcal{T} \in \{0, 1\}$, we can construct a contingency table, where $n_{i,j}$ represent the number of individuals with genotype $\mathcal{G} = i$ and phenotype $\mathcal{T} = j$, as illustrated in Table 1.

	$\mathcal{T} = 0$	$\mathcal{T} = 1$
$\mathcal{G} = 0$	$n_{0,0}$	$n_{0,1}$
$\mathcal{G} = 1$	$n_{1,0}$	$n_{1,1}$
$\mathcal{G} = 2$	$n_{2,0}$	$n_{2,1}$

Table 1: Contingency table for a binary trait and a bi-allelic locus.

Assuming co-dominance, the contingency table can be reduced to a 2x2 table by simply counting the number of alleles of type A and a associated to both traits: $n_{A,0}, n_{A,1}, n_{a,0}, n_{a,1}$: it is deduced from the general table with $n_{A,j} = 2n_{2,j} + n_{1,j}$ and $n_{a,j} = n_{1,j} + 2n_{0,j}$. When one allele is dominant, the contingency table also shrinks to a 2x2 table by pooling the counts of genotype $\mathcal{G} = 1$ with the genotype $\mathcal{G} = 2$ when A is dominant ($n_{D,j} = n_{2,j} + n_{1,j}$; $n_{R,j} = n_{0,j}$). Association is then simply tested by a χ^2 homogeneity test with 1 or 2 degrees of freedom depending on the table size. Larger contingency tables can be used to test for association for more than 2 alleles. Although the contingency table could, in theory, be extended to cases of non-binary phenotypes, it is in practice more convenient to re-express the problem in terms of linear regression.

Linear regression: additive genetic effect can be estimated by the following linear model:

$$T_i = a_0 + a_1 G_i + \varepsilon_i$$

This model can be used estimate both (i) the significance and strength of the correlation of a given allele with the phenotype and (ii) a_i , the amount of ad-

ditive effect of the allele to the trait. Techniques to estimate the a_i , such as least squares, are described in section 1. Although the basic version reported here assumes co-dominance, dominance can be explicitly addressed by setting the values of G_i adequately. Linear models handle elegantly cases of continuous traits, but are not well adapted when more than two alleles exist at a given locus.

Both contingency tables and linear models can be used to estimate the association of alleles at a given locus to the trait. In GWAS, one assesses correlations with as many as possible polymorphic loci of the genome. The hope is to find a haplotype that is significantly associated to the trait. As there is a very large number of loci and thus of statistical tests, the power to detect a single association even in large samples is weak. Thus, GWASs need by construction very large sample sizes to potentially detect significant associations. In brief, basic GWAS is based on counting co-occurrences of alleles and traits in individuals, ignoring their shared history.

One inherent challenge of measuring independent contribution of the loci to the phenotype is the presence of epistasis between the loci. A phenotype can be the results of the synergistic interaction of multiple alleles (see Figure 1b). Correlations can hide correlations. Attempts to include epistasis in the detection of association include the use of Mutual Information (MI), generalized to 3-partners [Ignac et al., 2014], 2 genetic partners with symmetrical roles and 1 phenotypic trait that is the value to be predicted. In this model, both loci contribute together to the trait: they have an additive component and an interaction term, that is reminiscent of the DCA assumptions (see section 2).

Although, erroneous associations could arise from multiple issues, one major annoyance is the stratification problem, that is the spurious association caused by population structuration [Lander and Schork, 1994, Pritchard et al., 2000, Price et al., 2006]. When a phenotype is mostly restricted to a subpopulation, all variants that characterize this subpopulation can be significantly associated with it. More generally, any correlation that is based on groups with and without a phenotype will suffer from the same bias, if there is some level of stratification. Therefore, like other correlated evolution methods based on counts of individuals, association mapping is biased by phylogenetic inertia, that can create non-relevant associations. Although there are several ways to handle this problem of stratification, one interesting method is to incorporate the genetic kinship between individuals in the model.

More specifically, individuals can be assigned to a genotype space, whose number of dimensions equals the number of genotyped loci. Their proxim-

ity in the genotype space relates to their kinship and their common ancestors [McVean, 2009], as individuals with recent ancestors are more similar genetically. A convenient way to summarize the genotype space is to transform the original space using PCA [Novembre and Stephens, 2008]. After the transformation, the first components of the new space are the ones explaining most of the variance, hence their name Principal Components, PC. Therefore, genetical proximity between individuals can be summarized (and often visualized) by only considering the first PCs that explain most of the genetic variance. One method [Price et al., 2006] correcting for stratification explicitly incorporates the positions of individuals, in the PCA space, within the linear model:

$$T_i = a_0 + a_1 G_i + \sum_j^n a_{j+1} \text{PC}_{i,j} + \varepsilon_i$$

where $\text{PC}_{i,j}$ is the value of the j^{th} PC of individual i . Interestingly, PCA is also used to visually inspect the homogeneity between the individuals and eventually remove outliers from the analysis [Purcell et al., 2007]. It should be mentioned that other multidimensional transformations, such as MDS (multidimensional scaling), are sometimes preferred over PCA.

Although GWAS were first developed for humans [Ozaki et al., 2002], they rapidly were applied to other organisms such as plants [Atwell et al., 2010], cattle [Mai et al., 2010] or even, more recently, bacteria [Chen and Shapiro, 2015]. Interestingly, in bacteria the impact of stratification is even stronger as recombination in bacterial genomes differs strongly from the meiotic recombination in Eukaryotes. In bacteria, recombination is assimilated to gene conversion, as it replaces only locally a piece of the genome, without affecting its backbone. Thus the kinship of bacterial genomes within species can be described by a tree, especially for species with a low level of recombination (the tree paradigm suffers major drawback when recombination is high or when divergence between lineages is large). Therefore, GWAS methods in bacteria were redesigned to correct for the genealogy of genomes, using methods almost identical to substitution mapping reported in section 2. However, there, all sites of the core genome are mapped on the tree together with the trait of interest. And, instead at looking at correlated evolution between all pairs of sites, the correlation is computed between each site and the trait [Collins and Didelot, 2018]. The observation that treeWAS, the recent GWAS version that is tree-aware, uses standard metric of correlated evolution that are precisely the same than the ones used to detect correlated evolution among sites in a genome, highlights again the theoretical and methodological proximity between classical genetics

and correlated evolution.

5 Conclusion

In this chapter, we have reviewed several models and methods used to characterize correlated evolution. We have divided the chapter in 3 sections, covering coevolution within morphological traits, coevolution within genetic traits and finally coevolution between genetic alleles and phenotypic traits. As we have seen, most methods we have described are highly similar in these three fields of applications. Even more, several methods can be directly applied to any types of traits, provided they are re-coded in the same abstraction. This unity in the methodologies fosters the common underlying framework of all these applications. We hope that this review will help readers to connect fields that could at first sight be considered as unrelated. Models and methods evolve, similar to living organisms. Consequently, they also share common ancestries, explaining their relatedness.

We have described two main schools of modelling correlated evolution that were developed in parallel. The first one simply considers sampled species, individuals or sequences, disregarding their shared history, and compute various metrics of correlation among the traits. A second one explicitly uses the shared history to compute correlation among evolutionary or segregation paths of the traits. We shall emphasize that, without any doubt, both frameworks have been successfully applied to many different questions, demonstrating their respective inner strengths. We would also like to stress that there may be good reasons to use one or the other. Practically, it can be hard to assess with confidence a phylogeny. Indeed, many problems can arise like: a) individuals within species have not a single genealogy for their their genome, making difficult to infer the tree sequence, b) inference can be entailed with large errors, especially for very divergent species, c) computation time can be too high in very large samples to infer a tree. Thus, in many cases, simply counting co-occurrences without looking at the phylogeny is an excellent choice. Conversely, when the genealogy can be assessed with confidence, computing correlations between evolutionary paths is powerful, as it follows the evolutionary processes rather solely their final outcomes. Typically on datasets of small size, the phylogenetic methods often perform better.

Interestingly, we have also seen that despite the change of traits one is willing to study (morphological, genetics, etc.), the fundamental principles and models of the methods remained invariant. However, as the data grow in number and

in quality, the fine implementation of the methods has been largely improved.

We have show that the method of correlating traits in biology to deduce some causality using prior knowledge between a predictor trait (e.g. a gene) and a induced one (e.g. a phenotype) is an old practice; this, despite the rampant ambiguity between correlation and causation. It is tempting to remind that formal statistical correlations were popularized under the impulse of biometricians [Galton, 1886, Pearson and Galton, 1895], suggesting that correlated evolution in biology has more ancient roots than the rise of genetics.

6 Acknowledgments

GA is supported by the INCEPTION program of the Pasteur Institute.

References

- E. Abouheif and D. J. Fairbairn. A Comparative Analysis of Allometry for Sexual Size Dimorphism: Assessing Rensch’s Rule. *The American Naturalist*, 149(3):540–562, 1997. ISSN 0003-0147. URL <https://www.jstor.org/stable/2463382>. Publisher: [University of Chicago Press, American Society of Naturalists].
- G. Achaz, A. Rodriguez-Verdugo, B. S. Gaut, and O. Tenaillon. The Reproducibility of Adaptation in the Light of Experimental Evolution with Whole Genome Sequencing. In C. R. Landry and N. Aubin-Horth, editors, *Ecological Genomics: Ecology and the Evolution of Genes and Genomes*, Advances in Experimental Medicine and Biology, pages 211–231. Springer Netherlands, Dordrecht, 2014. ISBN 978-94-007-7347-9. doi: 10.1007/978-94-007-7347-9_11. URL https://doi.org/10.1007/978-94-007-7347-9_11.
- S. Atwell, Y. S. Huang, B. J. Vilhjálmsson, G. Willems, M. Horton, Y. Li, D. Meng, A. Platt, A. M. Tarone, T. T. Hu, R. Jiang, N. W. Muliyati, X. Zhang, M. A. Amer, I. Baxter, B. Brachi, J. Chory, C. Dean, M. Debieu, J. de Meaux, J. R. Ecker, N. Faure, J. M. Kniskern, J. D. G. Jones, T. Michael, A. Nemri, F. Roux, D. E. Salt, C. Tang, M. Todesco, M. B. Traw, D. Weigel, P. Marjoram, J. O. Borevitz, J. Bergelson, and M. Nordborg. Genome-wide association study of 107 phenotypes in *Arabidopsis thaliana* inbred lines. *Nature*, 465(7298):627–631, June 2010. ISSN 1476-4687. doi: 10.1038/nature08800. URL <https://www.nature.com/articles/nature08800>. Number: 7298 Publisher: Nature Publishing Group.

- C. Baldassi, M. Zamparo, C. Feinauer, A. Procaccini, R. Zecchina, M. Weigt, and A. Pagnani. Fast and accurate multivariate Gaussian modeling of protein families: predicting residue contacts and protein-interaction partners. *PLoS ONE*, 9(3):e92721, 2014. ISSN 1932-6203. doi: 10.1371/journal.pone.0092721.
- D. Barker and M. Pagel. Predicting functional gene links from phylogenetic-statistical analyses of whole genomes. *PLoS Comput. Biol.*, 1(1):e3, June 2005. ISSN 1553-734X. doi: 10.1371/journal.pcbi.0010003.
- D. Barker, A. Meade, and M. Pagel. Constrained models of evolution lead to improved prediction of functional linkage from correlated gain and loss of genes. *Bioinformatics*, 23(1):14–20, Jan. 2007. ISSN 1367-4811. doi: 10.1093/bioinformatics/btl558.
- N. H. Barton, A. M. Etheridge, and A. Véber. The infinitesimal model: Definition, derivation, and implications. *Theoretical Population Biology*, 118:50–73, Dec. 2017. ISSN 0040-5809. doi: 10.1016/j.tpb.2017.06.001. URL <http://www.sciencedirect.com/science/article/pii/S0040580917300886>.
- A. Behdenna, J. Pothier, S. S. Abby, A. Lambert, and G. Achaz. Testing for Independence between Evolutionary Processes. *Syst. Biol.*, 65(5):812–823, Sept. 2016. ISSN 1076-836X. doi: 10.1093/sysbio/syw004.
- A.-F. Bitbol. Inferring interaction partners from protein sequences using mutual information. *PLoS Computational Biology*, 14(11):e1006401, Nov. 2018. ISSN 1553-7358. doi: 10.1371/journal.pcbi.1006401. URL <https://journals.plos.org/ploscompbiol/article?id=10.1371/journal.pcbi.1006401>. Publisher: Public Library of Science.
- S. P. Blomberg, T. Garland, and A. R. Ives. Testing for phylogenetic signal in comparative data: behavioral traits are more labile. *Evolution*, 57(4):717–745, Apr. 2003. ISSN 0014-3820. doi: 10.1111/j.0014-3820.2003.tb00285.x.
- R. Champeimont, E. Laine, S.-W. Hu, F. Penin, and A. Carbone. Coevolution analysis of Hepatitis C virus genome to identify the structural and functional dependency network of viral proteins. *Sci Rep*, 6(1):1–20, May 2016. ISSN 2045-2322. doi: 10.1038/srep26401. URL <https://www.nature.com/articles/srep26401>. Number: 1 Publisher: Nature Publishing Group.
- P. E. Chen and B. J. Shapiro. The advent of genome-wide association studies for bacteria. *Current Opinion in Microbiology*, 25:17–24, June 2015. ISSN 1369-5274. doi: 10.1016/j.mib.2015.03.002. URL <http://www.sciencedirect.com/science/article/pii/S1369527415000375>.

- J. M. Cheverud, M. M. Dow, and W. Leutenegger. The quantitative assessment of phylogenetic constraints in comparative analyses: sexual dimorphism in body weight among primates. *Evolution*, 39(6):1335–1351, Nov. 1985. ISSN 1558-5646. doi: 10.1111/j.1558-5646.1985.tb05699.x.
- D. K. Chiu and T. Kolodziejczak. Inferring consensus structure from nucleic acid sequences. *Comput. Appl. Biosci.*, 7(3):347–352, July 1991. ISSN 0266-7061. doi: 10.1093/bioinformatics/7.3.347.
- M. Cobb. 60 years ago, Francis Crick changed the logic of biology. *PLoS Biol.*, 15(9):e2003243, Sept. 2017. ISSN 1545-7885. doi: 10.1371/journal.pbio.2003243.
- O. Cohen, N. D. Rubinstein, A. Stern, U. Gophna, and T. Pupko. A likelihood framework to analyse phyletic patterns. *Philos. Trans. R. Soc. Lond., B, Biol. Sci.*, 363(1512):3903–3911, Dec. 2008. ISSN 1471-2970. doi: 10.1098/rstb.2008.0177.
- O. Cohen, H. Ashkenazy, D. Burstein, and T. Pupko. Uncovering the co-evolutionary network among prokaryotic genes. *Bioinformatics*, 28(18):i389–i394, Sept. 2012. ISSN 1367-4811. doi: 10.1093/bioinformatics/bts396.
- O. Cohen, H. Ashkenazy, E. Levy Karin, D. Burstein, and T. Pupko. CoPAP: Coevolution of presence-absence patterns. *Nucleic Acids Res.*, 41(Web Server issue):W232–237, July 2013. ISSN 1362-4962. doi: 10.1093/nar/gkt471.
- C. Collins and X. Didelot. A phylogenetic method to perform genome-wide association studies in microbes that accounts for population structure and recombination. *PLOS Computational Biology*, 14(2):e1005958, Feb. 2018. ISSN 1553-7358. doi: 10.1371/journal.pcbi.1005958. URL <https://journals.plos.org/ploscompbiol/article?id=10.1371/journal.pcbi.1005958>. Publisher: Public Library of Science.
- N. Cooper and A. Purvis. Body size evolution in mammals: complexity in tempo and mode. *Am. Nat.*, 175(6):727–738, June 2010. ISSN 1537-5323. doi: 10.1086/652466.
- D. de Juan, F. Pazos, and A. Valencia. Emerging methods in protein co-evolution. *Nat. Rev. Genet.*, 14(4):249–261, Apr. 2013. ISSN 1471-0064. doi: 10.1038/nrg3414.
- E. De Leonardis, B. Lutz, S. Ratz, S. Cocco, R. Monasson, A. Schug, and M. Weigt. Direct-Coupling Analysis of nucleotide coevolution facilitates

- RNA secondary and tertiary structure prediction. *Nucleic Acids Res.*, 43 (21):10444–10455, Dec. 2015. ISSN 1362-4962. doi: 10.1093/nar/gkv932.
- L. Dib and A. Carbone. Protein Fragments: Functional and Structural Roles of Their Coevolution Networks. *PLOS ONE*, 7(11):e48124, Nov. 2012. ISSN 1932-6203. doi: 10.1371/journal.pone.0048124. URL <https://journals.plos.org/plosone/article?id=10.1371/journal.pone.0048124>. Publisher: Public Library of Science.
- L. Dib, D. Silvestro, and N. Salamin. Evolutionary footprint of coevolving positions in genes. *Bioinformatics*, 30(9):1241–1249, May 2014. ISSN 1367-4811. doi: 10.1093/bioinformatics/btu012.
- J. Dutheil and N. Galtier. Detecting groups of coevolving positions in a molecule: a clustering approach. *BMC Evol. Biol.*, 7:242, 2007. ISSN 1471-2148. doi: 10.1186/1471-2148-7-242.
- J. Dutheil, T. Pupko, A. Jean-Marie, and N. Galtier. A model-based approach for detecting coevolving positions in a molecule. *Mol. Biol. Evol.*, 22(9):1919–1928, Sept. 2005. ISSN 0737-4038. doi: 10.1093/molbev/msi183.
- J. Y. Dutheil. Detecting coevolving positions in a molecule: why and how to account for phylogeny. *Brief. Bioinformatics*, 13(2):228–243, Mar. 2012. ISSN 1477-4054. doi: 10.1093/bib/bbr048.
- J. Y. Dutheil, F. Jossinet, and E. Westhof. Base pairing constraints drive structural epistasis in ribosomal RNA sequences. *Mol. Biol. Evol.*, 27(8):1868–1876, Aug. 2010. ISSN 1537-1719. doi: 10.1093/molbev/msq069.
- M. Ekeberg, C. Lövkvist, Y. Lan, M. Weigt, and E. Aurell. Improved contact prediction in proteins: using pseudolikelihoods to infer Potts models. *Phys Rev E Stat Nonlin Soft Matter Phys*, 87(1):012707, Jan. 2013. ISSN 1550-2376. doi: 10.1103/PhysRevE.87.012707.
- D. J. Fairbairn. Allometry for Sexual Size Dimorphism: Pattern and Process in the Coevolution of Body Size in Males and Females. *Annu. Rev. Ecol. Syst.*, 28(1):659–687, Nov. 1997. ISSN 0066-4162. doi: 10.1146/annurev.ecolsys.28.1.659. URL <https://www.annualreviews.org/doi/10.1146/annurev.ecolsys.28.1.659>. Publisher: Annual Reviews.
- M. A. Fares and S. A. A. Travers. A novel method for detecting intramolecular coevolution: adding a further dimension to selective constraints analyses.

- Genetics*, 173(1):9–23, May 2006. ISSN 0016-6731. doi: 10.1534/genetics.105.053249.
- J. Felsenstein. Maximum-likelihood estimation of evolutionary trees from continuous characters. *Am J Hum Genet*, 25(5):471–492, Sept. 1973. ISSN 0002-9297. URL <https://www.ncbi.nlm.nih.gov/pmc/articles/PMC1762641/>.
- J. Felsenstein. Evolutionary trees from DNA sequences: a maximum likelihood approach. *J. Mol. Evol.*, 17(6):368–376, 1981. ISSN 0022-2844.
- J. Felsenstein. Phylogenies and the Comparative Method. *The American Naturalist*, 125(1):1–15, 1985. ISSN 0003-0147. URL <https://www.jstor.org/stable/2461605>. Publisher: [University of Chicago Press, American Society of Naturalists].
- J. Felsenstein. *Inferring Phylogenies*. Sinauer Associates, 2 edition, Sept. 2003. ISBN 0-87893-177-5.
- M. Figliuzzi, H. Jacquier, A. Schug, O. Tenaillon, and M. Weigt. Coevolutionary Landscape Inference and the Context-Dependence of Mutations in Beta-Lactamase TEM-1. *Mol. Biol. Evol.*, 33(1):268–280, Jan. 2016. ISSN 1537-1719. doi: 10.1093/molbev/msv211.
- N. Galtier and J. Dutheil. Coevolution within and between genes. *Genome Dyn*, 3:1–12, 2007. ISSN 1660-9263. doi: 10.1159/000107599.
- F. Galton. Regression Towards Mediocrity in Hereditary Stature. Jan. 1886. doi: 10.2307/2841583. URL <https://zenodo.org/record/1449548#.XsfkzJrRaQA>.
- J. L. Gittleman. Carnivore body size: Ecological and taxonomic correlates. *Oecologia*, 67(4):540–554, Dec. 1985. ISSN 1432-1939. doi: 10.1007/BF00790026.
- C. S. Goh, A. A. Bogan, M. Joachimiak, D. Walther, and F. E. Cohen. Coevolution of proteins with their interaction partners. *J. Mol. Biol.*, 299(2): 283–293, June 2000. ISSN 0022-2836. doi: 10.1006/jmbi.2000.3732.
- A. Grafen. The phylogenetic regression. *Philos. Trans. R. Soc. Lond., B, Biol. Sci.*, 326(1233):119–157, Dec. 1989. ISSN 0962-8436. doi: 10.1098/rstb.1989.0106.
- U. Göbel, C. Sander, R. Schneider, and A. Valencia. Correlated mutations and residue contacts in proteins. *Proteins*, 18(4):309–317, Apr. 1994. ISSN 0887-3585. doi: 10.1002/prot.340180402.

- P. H. Harvey and M. D. Pagel. *The Comparative Method In Evolutionary Biology*. Oxford University Press, U.S.A., Oxford ; New York, June 1991. ISBN 978-0-19-854640-5.
- R. W. Holley, J. Apgar, G. A. Everett, J. T. Madison, M. Marquisee, S. H. Merrill, J. R. Penswick, and A. Zamir. Structure of a ribonucleic acid. *Science*, 147(3664):1462–1465, Mar. 1965. ISSN 0036-8075. doi: 10.1126/science.147.3664.1462.
- T. A. Hopf, L. J. Colwell, R. Sheridan, B. Rost, C. Sander, and D. S. Marks. Three-Dimensional Structures of Membrane Proteins from Genomic Sequencing. *Cell*, 149(7):1607–1621, June 2012. ISSN 0092-8674, 1097-4172. doi: 10.1016/j.cell.2012.04.012. URL [https://www.cell.com/cell/abstract/S0092-8674\(12\)00509-0](https://www.cell.com/cell/abstract/S0092-8674(12)00509-0). Publisher: Elsevier.
- T. M. Ignac, A. Skupin, N. A. Sakhanenko, and D. J. Galas. Discovering Pair-Wise Genetic Interactions: An Information Theory-Based Approach. *PLOS ONE*, 9(3):e92310, Mar. 2014. ISSN 1932-6203. doi: 10.1371/journal.pone.0092310. URL <https://journals.plos.org/plosone/article?id=10.1371/journal.pone.0092310>. Publisher: Public Library of Science.
- K. M. Kay, P. A. Reeves, R. G. Olmstead, and D. W. Schemske. Rapid speciation and the evolution of hummingbird pollination in neotropical *Costus* subgenus *Costus* (Costaceae): evidence from nrDNA ITS and ETS sequences. *American Journal of Botany*, 92(11):1899–1910, 2005. ISSN 1537-2197. doi: 10.3732/ajb.92.11.1899. URL <https://bsapubs.onlinelibrary.wiley.com/doi/abs/10.3732/ajb.92.11.1899>. eprint: <https://bsapubs.onlinelibrary.wiley.com/doi/pdf/10.3732/ajb.92.11.1899>.
- S. Kryazhimskiy, J. Dushoff, G. A. Bazykin, and J. B. Plotkin. Prevalence of epistasis in the evolution of influenza A surface proteins. *PLoS Genet.*, 7(2): e1001301, Feb. 2011. ISSN 1553-7404. doi: 10.1371/journal.pgen.1001301.
- E. Laine, Y. Karami, and A. Carbone. GEMME: A Simple and Fast Global Epistatic Model Predicting Mutational Effects. *Mol Biol Evol*, 36(11):2604–2619, Nov. 2019. ISSN 0737-4038. doi: 10.1093/molbev/msz179. URL <https://academic.oup.com/mbe/article/36/11/2604/5548199>. Publisher: Oxford Academic.
- R. Lande, S. Engen, and B. Sæther. Spatial Scale of Population Synchrony: Environmental Correlation versus Dispersal and Density Regulation. *The*

- American Naturalist*, 154(3):271–281, Sept. 1999. ISSN 0003-0147. doi: 10.1086/303240. URL <https://www.journals.uchicago.edu/doi/full/10.1086/303240>. Publisher: The University of Chicago Press.
- E. S. Lander and N. J. Schork. Genetic dissection of complex traits. *Science*, 265(5181):2037–2048, Sept. 1994. ISSN 0036-8075, 1095-9203. doi: 10.1126/science.8091226. URL <https://science.sciencemag.org/content/265/5181/2037>. Publisher: American Association for the Advancement of Science Section: Articles.
- N. Lartillot. Interaction between Selection and Biased Gene Conversion in Mammalian Protein-Coding Sequence Evolution Revealed by a Phylogenetic Covariance Analysis. *Mol Biol Evol*, 30(2):356–368, Feb. 2013. ISSN 0737-4038. doi: 10.1093/molbev/mss231. URL <https://academic.oup.com/mbe/article/30/2/356/1015523>. Publisher: Oxford Academic.
- N. Lartillot and F. Delsuc. Joint Reconstruction of Divergence Times and Life-History Evolution in Placental Mammals Using a Phylogenetic Covariance Model. *Evolution*, 66(6):1773–1787, 2012. ISSN 1558-5646. doi: 10.1111/j.1558-5646.2011.01558.x. URL <https://onlinelibrary.wiley.com/doi/abs/10.1111/j.1558-5646.2011.01558.x>. eprint: <https://onlinelibrary.wiley.com/doi/pdf/10.1111/j.1558-5646.2011.01558.x>.
- N. Lartillot and R. Poujol. A phylogenetic model for investigating correlated evolution of substitution rates and continuous phenotypic characters. *Mol. Biol. Evol.*, 28(1):729–744, Jan. 2011. ISSN 1537-1719. doi: 10.1093/molbev/msq244.
- T. Lenormand. The evolution of sex dimorphism in recombination. *Genetics*, 163(2):811–822, Feb. 2003. ISSN 0016-6731.
- T. Lenormand and J. Dutheil. Recombination difference between sexes: a role for haploid selection. *PLoS Biol.*, 3(3):e63, Mar. 2005. ISSN 1545-7885. doi: 10.1371/journal.pbio.0030063.
- R. Lewontin. Building a science of population biology. In R. S. Singh and M. K. Uyenoyama, editors, *The Evolution of Population Biology*. Cambridge University Press, Jan. 2004. ISBN 978-1-139-44954-0.
- A. Long, G. Liti, A. Luptak, and O. Tenailon. Elucidating the molecular architecture of adaptation via evolve and resequence experiments. *Nature Reviews Genetics*, 16(10):567–582, Oct. 2015. ISSN 1471-0064. doi: 10.1038/

- nrg3937. URL <https://www.nature.com/articles/nrg3937>. Number: 10
Publisher: Nature Publishing Group.
- W. P. Maddison. A Method for Testing the Correlated Evolution of Two Binary Characters: Are Gains or Losses Concentrated on Certain Branches of a Phylogenetic Tree? *Evolution*, 44(3):539–557, 1990. ISSN 1558-5646. doi: 10.1111/j.1558-5646.1990.tb05937.x. URL <https://onlinelibrary.wiley.com/doi/abs/10.1111/j.1558-5646.1990.tb05937.x>. eprint: <https://onlinelibrary.wiley.com/doi/pdf/10.1111/j.1558-5646.1990.tb05937.x>.
- M. D. Mai, G. Sahana, F. B. Christiansen, and B. Guldbrandtsen. A genome-wide association study for milk production traits in Danish Jersey cattle using a 50K single nucleotide polymorphism chip. *J Anim Sci*, 88(11):3522–3528, Nov. 2010. ISSN 0021-8812. doi: 10.2527/jas.2009-2713. URL <https://academic.oup.com/jas/article/88/11/3522/4764149>. Publisher: Oxford Academic.
- D. S. Marks, L. J. Colwell, R. Sheridan, T. A. Hopf, A. Pagnani, R. Zecchina, and C. Sander. Protein 3D Structure Computed from Evolutionary Sequence Variation. *PLOS ONE*, 6(12):e28766, Dec. 2011. ISSN 1932-6203. doi: 10.1371/journal.pone.0028766. URL <https://journals.plos.org/plosone/article?id=10.1371/journal.pone.0028766>. Publisher: Public Library of Science.
- E. P. Martins. Estimating the Rate of Phenotypic Evolution from Comparative Data. *The American Naturalist*, 144(2):193–209, 1994. ISSN 0003-0147. URL <https://www.jstor.org/stable/2463156>. Publisher: [University of Chicago Press, American Society of Naturalists].
- E. P. Martins and T. F. Hansen. Phylogenies and the Comparative Method: A General Approach to Incorporating Phylogenetic Information into the Analysis of Interspecific Data. *The American Naturalist*, 149(4):646–667, 1997. ISSN 0003-0147. URL <https://www.jstor.org/stable/2463542>. Publisher: [University of Chicago Press, American Society of Naturalists].
- G. McVean. A Genealogical Interpretation of Principal Components Analysis. *PLOS Genetics*, 5(10):e1000686, Oct. 2009. ISSN 1553-7404. doi: 10.1371/journal.pgen.1000686. URL <https://journals.plos.org/plosgenetics/article?id=10.1371/journal.pgen.1000686>. Publisher: Public Library of Science.

- J. G. Mendel. Versuche über pflanzenhybriden (eng. experiments in plant hybridization). *Verhandlungen des naturforschenden Vereines in Brünn (ENG. Journal of the Royal Horticultural Society, 1901)*, 26:1–32., 1866.
- X. Meyer, L. Dib, D. Silvestro, and N. Salamin. Simultaneous Bayesian inference of phylogeny and molecular coevolution. *Proc. Natl. Acad. Sci. U.S.A.*, 116(11):5027–5036, 2019. ISSN 1091-6490. doi: 10.1073/pnas.1813836116.
- R. Moore. The "Rediscovery" of Mendel's Work. *Bioscene*, 27(2):13–24, 2001.
- F. Morcos, A. Pagnani, B. Lunt, A. Bertolino, D. S. Marks, C. Sander, R. Zecchina, J. N. Onuchic, T. Hwa, and M. Weigt. Direct-coupling analysis of residue coevolution captures native contacts across many protein families. *Proc. Natl. Acad. Sci. U.S.A.*, 108(49):E1293–1301, Dec. 2011. ISSN 1091-6490. doi: 10.1073/pnas.1111471108.
- T. H. Morgan. *The Theory of the Gene: 2D Ed.* Creative Media Partners, LLC, Oct. 2018. ISBN 978-0-343-29036-8. Google-Books-ID: dIqDAQAACAAJ.
- N. E. Morton. Sequential tests for the detection of linkage. *Am. J. Hum. Genet.*, 7(3):277–318, Sept. 1955. ISSN 0002-9297.
- E. Neher. How frequent are correlated changes in families of protein sequences? *Proc. Natl. Acad. Sci. U.S.A.*, 91(1):98–102, Jan. 1994. ISSN 0027-8424. doi: 10.1073/pnas.91.1.98.
- J. Novembre and M. Stephens. Interpreting principal component analyses of spatial population genetic variation. *Nature Genetics*, 40(5):646–649, May 2008. ISSN 1546-1718. doi: 10.1038/ng.139. URL <https://www.nature.com/articles/ng.139>. Number: 5 Publisher: Nature Publishing Group.
- D. R. Nyholt. All LODs Are Not Created Equal*. *The American Journal of Human Genetics*, 67(2):282–288, Aug. 2000. ISSN 0002-9297, 1537-6605. doi: 10.1086/303029. URL [https://www.cell.com/ajhg/abstract/S0002-9297\(07\)62639-1](https://www.cell.com/ajhg/abstract/S0002-9297(07)62639-1). Publisher: Elsevier.
- K. Ozaki, Y. Ohnishi, A. Iida, A. Sekine, R. Yamada, T. Tsunoda, H. Sato, H. Sato, M. Hori, Y. Nakamura, and T. Tanaka. Functional SNPs in the lymphotoxin- α gene that are associated with susceptibility to myocardial infarction. *Nature Genetics*, 32(4):650–654, Dec. 2002. ISSN 1546-1718. doi: 10.1038/ng1047. URL <https://www.nature.com/articles/ng1047z>. Number: 4 Publisher: Nature Publishing Group.

- M. Pagel. Detecting correlated evolution on phylogenies: a general method for the comparative analysis of discrete characters. *Proceedings of the Royal Society of London. Series B: Biological Sciences*, 255(1342):37–45, Jan. 1994. doi: 10.1098/rspb.1994.0006. URL <https://royalsocietypublishing.org/doi/10.1098/rspb.1994.0006>. Publisher: Royal Society.
- E. Paradis and J. Claude. Analysis of comparative data using generalized estimating equations. *J. Theor. Biol.*, 218(2):175–185, Sept. 2002. ISSN 0022-5193. doi: 10.1006/jtbi.2002.3066.
- F. Pazos and A. Valencia. Similarity of phylogenetic trees as indicator of protein-protein interaction. *Protein Eng.*, 14(9):609–614, Sept. 2001. ISSN 0269-2139. doi: 10.1093/protein/14.9.609.
- K. Pearson and F. Galton. VII. Note on regression and inheritance in the case of two parents. *Proceedings of the Royal Society of London*, 58(347-352):240–242, Jan. 1895. doi: 10.1098/rspl.1895.0041. URL <https://royalsocietypublishing.org/doi/10.1098/rspl.1895.0041>. Publisher: Royal Society.
- J. Pensar, S. Puranen, B. Arnold, N. MacAlasdair, J. Kuronen, G. Tonkin-Hill, M. Pesonen, Y. Xu, A. Sipola, L. Sánchez-Busó, J. A. Lees, C. Chewapreecha, S. D. Bentley, S. R. Harris, J. Parkhill, N. J. Croucher, and J. Corander. Genome-wide epistasis and co-selection study using mutual information. *Nucleic Acids Res*, 47(18):e112–e112, Oct. 2019. ISSN 0305-1048. doi: 10.1093/nar/gkz656. URL <https://academic.oup.com/nar/article/47/18/e112/5541093>. Publisher: Oxford Academic.
- P. C. Phillips. Epistasis — the essential role of gene interactions in the structure and evolution of genetic systems. *Nat Rev Genet*, 9(11):855–867, Nov. 2008. ISSN 1471-0064. doi: 10.1038/nrg2452. URL <https://www.nature.com/articles/nrg2452>. Number: 11 Publisher: Nature Publishing Group.
- D. D. Pollock, W. R. Taylor, and N. Goldman. Coevolving protein residues: maximum likelihood identification and relationship to structure. *J. Mol. Biol.*, 287(1):187–198, Mar. 1999. ISSN 0022-2836. doi: 10.1006/jmbi.1998.2601.
- A. L. Price, N. J. Patterson, R. M. Plenge, M. E. Weinblatt, N. A. Shadick, and D. Reich. Principal components analysis corrects for stratification in genome-wide association studies. *Nature Genetics*, 38(8):904–909, Aug. 2006. ISSN 1546-1718. doi: 10.1038/ng1847. URL <https://www.nature.com/articles/ng1847>. Number: 8 Publisher: Nature Publishing Group.

- J. K. Pritchard, M. Stephens, N. A. Rosenberg, and P. Donnelly. Association Mapping in Structured Populations. *The American Journal of Human Genetics*, 67(1):170–181, July 2000. ISSN 0002-9297. doi: 10.1086/302959. URL <http://www.sciencedirect.com/science/article/pii/S0002929707624422>.
- S. Puranen, M. Pesonen, J. Pensar, Y. Y. Xu, J. A. Lees, S. D. Bentley, N. J. Croucher, and J. Corander. SuperDCA for genome-wide epistasis analysis. *Microbial Genomics*, 4(6):e000184, 2018. ISSN . doi: 10.1099/mgen.0.000184. URL <https://www.microbiologyresearch.org/content/journal/mgen/10.1099/mgen.0.000184>. Publisher: Microbiology Society,.
- S. Purcell, B. Neale, K. Todd-Brown, L. Thomas, M. A. R. Ferreira, D. Bender, J. Maller, P. Sklar, P. I. W. de Bakker, M. J. Daly, and P. C. Sham. PLINK: A Tool Set for Whole-Genome Association and Population-Based Linkage Analyses. *The American Journal of Human Genetics*, 81(3):559–575, Sept. 2007. ISSN 0002-9297. doi: 10.1086/519795. URL <http://www.sciencedirect.com/science/article/pii/S0002929707613524>.
- B. Rensch. *Die Abhängigkeit der relativen Sexualdifferenz von der Körpergröße*, volume 1. Bonner zoologische Beiträge, 1950.
- M. Ridley. *The Explanation of Organic Diversity: The Comparative Method and Adaptations for Mating*. Oxford University Press, Oxford : Oxford ; New York, Dec. 1983. ISBN 978-0-19-857597-9.
- I. N. Shindyalov, N. A. Kolchanov, and C. Sander. Can three-dimensional contacts in protein structures be predicted by analysis of correlated mutations? *Protein Eng.*, 7(3):349–358, Mar. 1994. ISSN 0269-2139. doi: 10.1093/protein/7.3.349.
- H. Szurmant and M. Weigt. Inter-residue, inter-protein and inter-family coevolution: bridging the scales. *Curr. Opin. Struct. Biol.*, 50:26–32, 2018. ISSN 1879-033X. doi: 10.1016/j.sbi.2017.10.014.
- D. Talavera, S. C. Lovell, and S. Whelan. Covariation Is a Poor Measure of Molecular Coevolution. *Mol. Biol. Evol.*, 32(9):2456–2468, Sept. 2015. ISSN 1537-1719. doi: 10.1093/molbev/msv109.
- E. R. Tillier and R. A. Collins. High apparent rate of simultaneous compensatory base-pair substitutions in ribosomal RNA. *Genetics*, 148(4):1993–2002, Apr. 1998. ISSN 0016-6731.

- E. R. M. Tillier and R. A. Collins. Neighbor Joining and Maximum Likelihood with RNA Sequences: Addressing the Interdependence of Sites. *Mol Biol Evol*, 12(1):7–7, Jan. 1995. ISSN 0737-4038. doi: 10.1093/oxfordjournals.molbev.a040195. URL <https://academic.oup.com/mbe/article/12/1/7/999573>. Publisher: Oxford Academic.
- P. Tufféry and P. Darlu. Exploring a phylogenetic approach for the detection of correlated substitutions in proteins. *Mol. Biol. Evol.*, 17(11):1753–1759, Nov. 2000. ISSN 0737-4038. doi: 10.1093/oxfordjournals.molbev.a026273.
- L. Van Valen. A New Evolutionary Law. *Evol. Theory*, 1(1):1–30, July 1973.
- J. A. G. M. d. Visser and J. Krug. Empirical fitness landscapes and the predictability of evolution. *Nat Rev Genet*, 15(7):480–490, July 2014. ISSN 1471-0064. doi: 10.1038/nrg3744. URL <https://www.nature.com/articles/nrg3744>. Number: 7 Publisher: Nature Publishing Group.
- M. Weigt, R. A. White, H. Szurmant, J. A. Hoch, and T. Hwa. Identification of direct residue contacts in protein–protein interaction by message passing. *PNAS*, 106(1):67–72, Jan. 2009. ISSN 0027-8424, 1091-6490. doi: 10.1073/pnas.0805923106. URL <https://www.pnas.org/content/106/1/67>. Publisher: National Academy of Sciences Section: Physical Sciences.
- E. Westhof and P. Auffinger. Transfer RNA structure. In *eLS*. American Cancer Society, 2012. ISBN 978-0-470-01590-2. doi: 10.1002/9780470015902.a0000527.pub2. URL <https://onlinelibrary.wiley.com/doi/abs/10.1002/9780470015902.a0000527.pub2>. eprint: <https://onlinelibrary.wiley.com/doi/pdf/10.1002/9780470015902.a0000527.pub2>.
- M. E. J. Woolhouse, J. P. Webster, E. Domingo, B. Charlesworth, and B. R. Levin. Biological and biomedical implications of the co-evolution of pathogens and their hosts. *Nat Genet*, 32(4):569–577, Dec. 2002. ISSN 1546-1718. doi: 10.1038/ng1202-569. URL <https://www.nature.com/articles/ng1202-569>. Number: 4 Publisher: Nature Publishing Group.
- S. Wright. The roles of mutation, inbreeding, crossbreeding and selection in evolution. In *Proceedings of the Sixth International Congress on Genetics*, volume 1, page 356–366, 1932.
- Z. Yang. *Computational Molecular Evolution*. Oxford University Press, Oxford, Dec. 2006. ISBN 978-0-19-856702-8.

- C.-H. Yeang. Identifying coevolving partners from paralogous gene families. *Evol. Bioinform. Online*, 4:97–107, Apr. 2008. ISSN 1176-9343. doi: 10.4137/ebo.s621.
- C.-H. Yeang and D. Haussler. Detecting coevolution in and among protein domains. *PLoS Comput. Biol.*, 3(11):e211, Nov. 2007. ISSN 1553-7358. doi: 10.1371/journal.pcbi.0030211.
- C.-H. Yeang, J. F. J. Darot, H. F. Noller, and D. Haussler. Detecting the coevolution of biosequences—an example of RNA interaction prediction. *Mol. Biol. Evol.*, 24(9):2119–2131, Sept. 2007. ISSN 0737-4038. doi: 10.1093/molbev/msm142.
- X. Yi and A. M. Dean. Adaptive Landscapes in the Age of Synthetic Biology. *Mol Biol Evol*, 36(5):890–907, May 2019. ISSN 0737-4038. doi: 10.1093/molbev/msz004. URL <https://academic.oup.com/mbe/article/36/5/890/5290102>. Publisher: Oxford Academic.

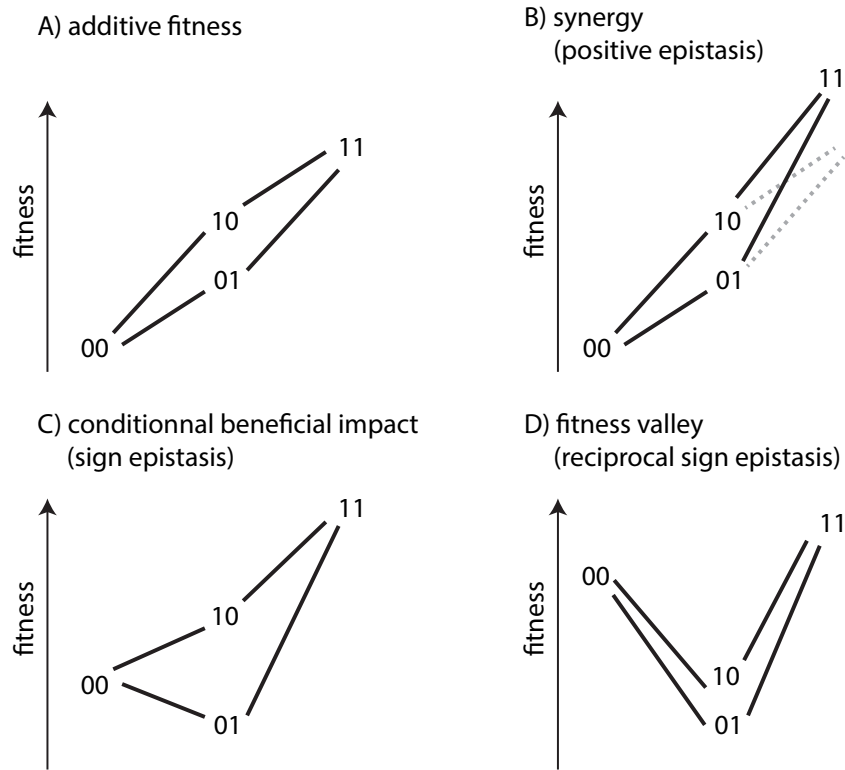


Figure 1: Four examples of fitness landscapes with 2 binary traits, resulting in four possible combinations. The height of a combination represents its fitness. A) When the fitness difference of the double mutant compared to the reference, is simply the sum of each mutation, there is no dependency between the two mutations. The landscape is named additive and the two traits evolve independently. B) When the fitness improvement of the double mutant is more than the additive case, there is a synergistic effect of both mutations. C) The mutation of the second trait is deleterious in the reference ($00 \rightarrow 01$) but beneficial once the first trait has mutated ($10 \rightarrow 11$). D) Both traits are deleterious when mutated on their own but compensate each other in the double mutant.

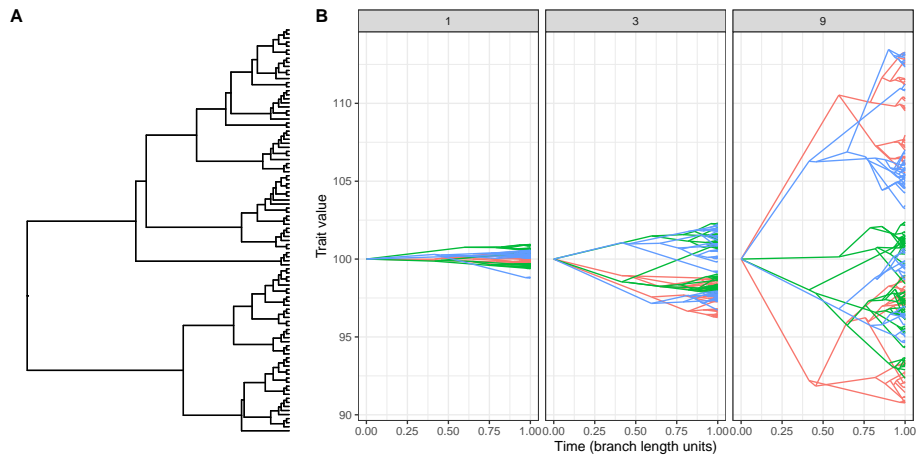


Figure 2: Evolution of a continuous trait under a Brownian motion along a phylogeny. A) A 100 species random phylogeny used for simulation. B) Simulations under the phylogeny depicted in A) using a Brownian motion with variance equal to 1, 3 or 9. Three independent replicates are displayed with three distinct colors in each case. Note the emergent co-variation in the traits, that is only due to the shared phylogeny.

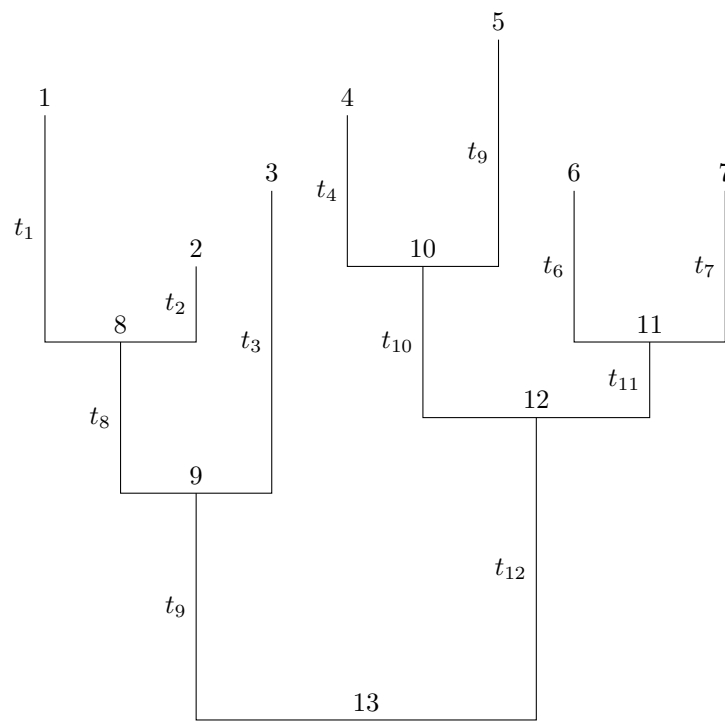


Figure 3: Example rooted phylogeny with node labels and branch lengths

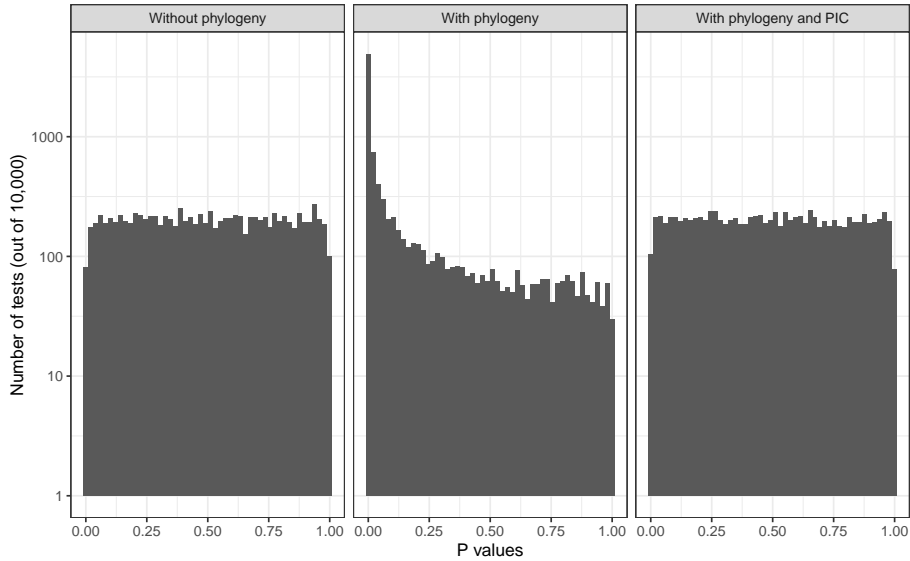


Figure 4: P value distribution of Kendall's correlation test on two continuous traits simulated independently. Left: without phylogeny or a star-like phylogeny (no shared history). Center: with phylogeny. Right: with phylogeny and correction using phylogenetic independent contrasts (PIC). 10,000 simulations were performed in each case, with a 100 pairs of points.

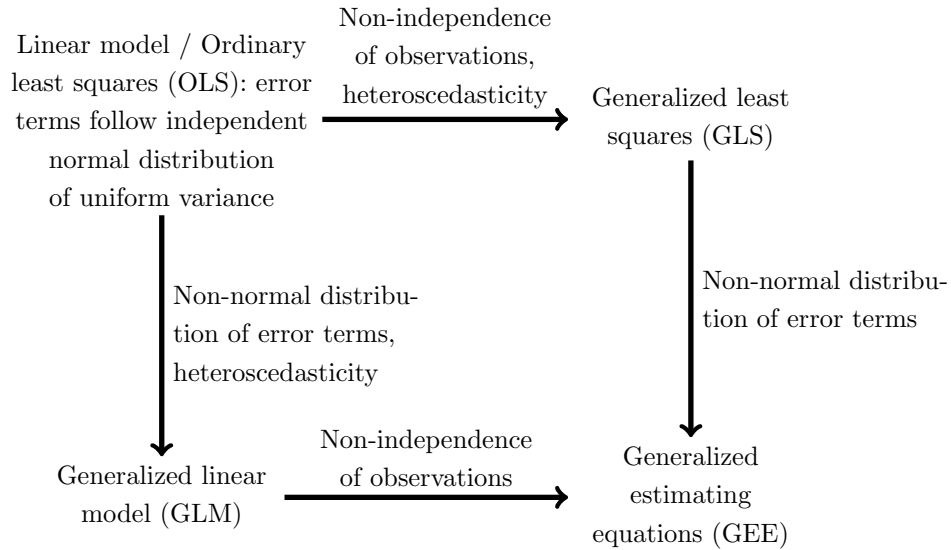
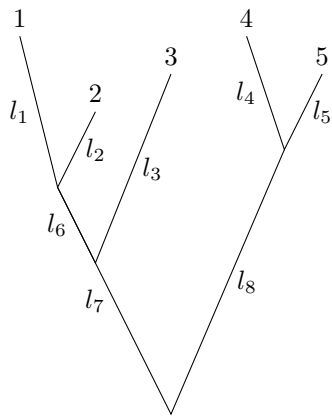


Figure 5: The linear modeling framework and its extensions



$$V_{\text{brownian}} = \sigma^2 \begin{pmatrix} l_1 + l_6 + l_7 & l_6 + l_7 & l_7 & 0 & 0 \\ l_6 + l_7 & l_2 + l_6 + l_7 & l_7 & 0 & 0 \\ l_7 & l_7 & l_3 + l_7 & 0 & 0 \\ 0 & 0 & 0 & l_4 + l_8 & l_8 \\ 0 & 0 & 0 & l_8 & l_5 + l_8 \end{pmatrix}$$

Figure 6: Variance-covariance matrix obtained from a rooted phylogeny with branch lengths, assuming a Brownian motion for the trait evolution. σ^2 is the intrinsic variance of the continuous trait.

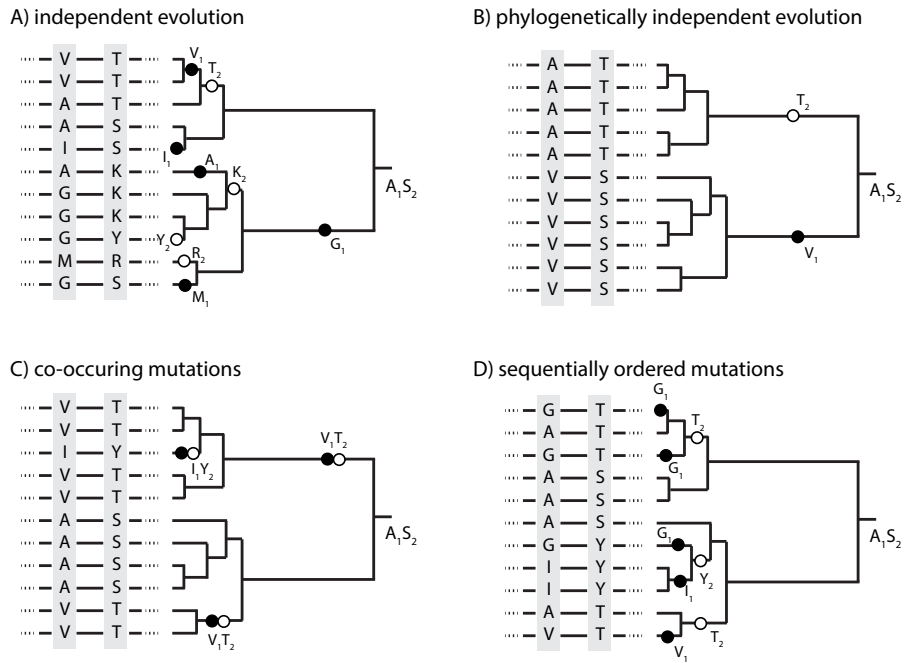


Figure 7: Four possible outcomes of the comparison between two columns of an alignment. The grey area brings the focus to two columns of a larger alignment. The phylogenetic tree on the side illustrates the process of substitution mapping on the tree. Ancestral state is given at the root, mutations at the first site are displayed by black disks, while mutations at the second site by empty circles. A) For most pairs of sites, no correlated variation is observed neither in the alignment nor in the tree. B) Although the two pairs evolve independently, the phylogenetic inertia can mimic patterns of correlated variation in the alignment. The pattern would only be statistically significant for MI-like methods when phylogeny is ignored. C) A pattern of co-variation corresponding to co-substitutions in the tree, suggestive of a strong reciprocal interaction between both sites. D) A pattern of correlated evolution with a time lag between the first mutation and the following one, suggestive of an asymmetrical induction of mutations at site 2 on mutations at site 1.

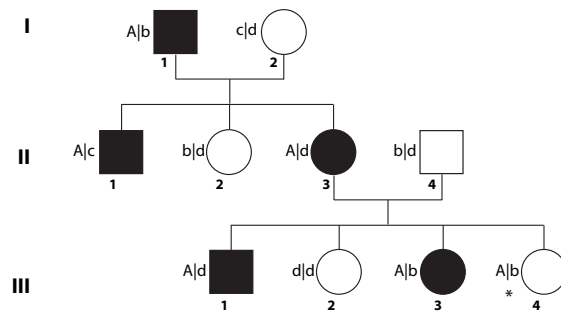


Figure 8: This pedigree reports the transmission of a phenotypic trait segregating through 3 generations, labeled I to III. Males (squares) and females (circles) are colored in black when they show the phenotype. On the left of each individual, we report the observed genotype at a focal locus. Here, the suspicion is that the A allele at the locus co-segregates with the phenotype.